IEEE Access
Multidisciplinary | Rapid Review | Open Access Journal

Received July 14, 2019, accepted July 26, 2019, date of publication August 9, 2019, date of current version August 22, 2019.

Digital Object Identifier 10.1109/ACCESS.2019.2934143

Prospect of Using Artificial Intelligence for Microwave Nondestructive Testing Technique: A Review

NAWAF H. M. M. SHRIFAN[1,2], MUHAMMAD FIRDAUS AKBAR[1], (Member, IEEE), AND NOR ASHIDI MAT ISA[1]

[1]School of Electrical and Electronic Engineering, Universiti Sains Malaysia, Penang 14300, Malaysia
[2]Faculty of Oil and Minerals, University of Aden, Shabwah, Yemen

Corresponding author: Nor Ashidi Mat Isa (ashidi@usm.my)

This work was supported by the USM Short-Term under Grant 304/PELECT/6315298.

ABSTRACT The development in materials technology has produced stronger, lighter, stiffer, and more durable electrically insulating composites which are replacing metals in many applications. These composites require alternative inspection techniques because the conventional nondestructive testing (NDT) techniques such as thermography, eddy currents, ultrasonic, X-ray and magnetic particles have limitations of inspecting them. Microwave NDT technique employing open-ended rectangular waveguides (OERW) has emerged as a promising approach to detect the defects in both metal and composite materials. Despite its promising results over conventional NDT techniques, OERW microwave NDT technique has shown numerous limitations in terms of poor spatial resolution due to the stand-off distance variations, inspection area irregularities and quantitative estimation in imaging the size of defects. Microwave NDT employing OERW in conjunction with robust artificial intelligence approaches have tremendous potential and viability for evaluating composite structures for the purpose mentioned here. Artificial intelligence techniques with signal processing techniques are highly possible to enhance the efficiency and resolution of microwave NDT technique because the impact of artificial intelligence approaches is proven in various conventional NDT techniques. This paper provides a comprehensive review of NDT techniques as well as the prospect of using artificial intelligence approaches in microwave NDT technique with regards to other conventional NDT techniques.

INDEX TERMS Microwave nondestructive testing, open-ended rectangular waveguides, artificial intelligence.

I. INTRODUCTION

The developments of imaging techniques for investigating physically inaccessible objects have been a topic of research for many years and have found widespread applications in the field of nondestructive testing (NDT). Nondestructive testing (NDT) is defined as a practice of evaluating the change in various properties of a material such as delamination, corrosion, cracks, and fatigue including internal flaw or metallurgical condition without interfering in any way the integrity of the material or its suitability for service [1]. Regular inspection evaluating the integrity of the system is mandatory by using NDT to prevent serious system failures, which have several adverse consequences including the risk to the safety of site personnel, damage to the environment, and an economic impact in terms of the maintenance cost and production lost. NDT plays a crucial role in many industrial applications especially in aerospace, power generation, petrochemical, railway and automotive. The NDT inspections to assess the damage to structure or parts of the system is crucial for the saving of the maintenance cost, improving the safety and reliability of the entire system [2].

There is a wide range of commonly used NDT methods and well established in the industry such as thermography inspection, ultrasonic inspection, eddy currents testing, X-ray and magnetic particles inspection [3], [4]. The choice

The associate editor coordinating the review of this manuscript and approving it for publication was Orazio Gambino.

between these techniques is based on their advantages and disadvantages with considering the safety, operational cost and their efficiency with the material to be inspected. For instance, ultrasonic inspection is not capable of penetrating highly porous materials and requiring extensive data interpretation [5]. Although the laser ultrasonic performs the non-contact inspection without the couplant, its performance is degraded when inspecting highly porous materials [6]. Moreover, laser ultrasonic simultaneously generates various waves (e.g. shear, longitudinal waves, Rayleigh and Lamb waves) which complicate the signal analysis [7]. The eddy current testing is extensively used in industry for surface crack and corrosion detection but this method does not work well when inspecting low-loss dielectric materials due to penetration limitation of low-frequency electromagnetic waves [8].

The demands of composite materials replacing or coated with metals in many applications require alternative inspection technique since conventional NDT technique does not work properly when inspecting composite materials due to field penetration limitations. Composite materials become popular due to their stability, strength and lightweight characteristics, replacing metals in many applications such as power plant, aerospace and automotive industries. The performances of these materials are affected due to aging and the cyclic process by various defects such as corrosion, cracks on metal substrate undercoating, delamination between coatings and the metal substrate. Microwave nondestructive testing (MNDT) technique is well suited for inspecting the composite materials since the electromagnetic waves at microwave frequencies hold the prospect of providing better inspection resolution for composite materials [9].

Microwave signals, unlike ultrasonic and acoustic signals, are capable to penetrates inside composite material such as dielectric insulations and interact with their inner structure and sensitive to changes associated with boundary interfaces makes them a very attractive candidate for composite inspection. Several microwave techniques have been reported for composite inspection. Despite their promising results, the conventional microwave based techniques face several challenges such as data complexity, poor quality of the spatial image and blurred defect shape due to the stand-off distance variations and optimal frequency point selection which degrade the geometrical measurements of defects [5], [10]. Therefore, the emerging of soft computing techniques makes it possible to handle these challenges due to the development of intelligent systems such as machine learning-based techniques. The high capability of machine learning techniques to solve complex data make it applicable to handle the microwave data complexity and small variations as well as to improve the sensitivity of the sensor and spatial image resolution [11].

The trend of using artificial intelligence (AI) for defects detection and identification is recommended in some researches such as an artificial intelligence-based machine learning has been used to build a classification system to automate defects identification during fabrication or in service as well as improves the quality of NDT inspection [12]. Despite the promising future of both MNDT and AI as separate techniques, the current attempts to hybridize them together have great potential to overcome the mentioned challenges.

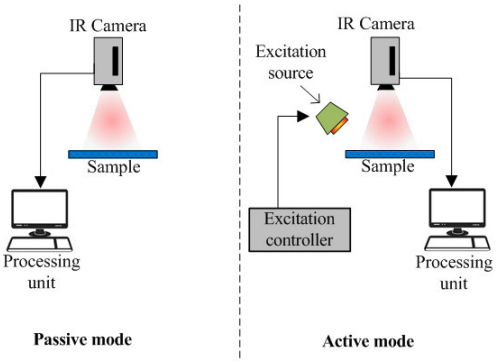

FIGURE 1. Schematic diagrams of thermography NDT passive and active modes.

A comprehensive review of NDT techniques as well as the prospect of using artificial intelligence approaches in microwave NDT technique is reviewed and presented in this paper. Conventional NDT techniques such as thermography, eddy current, ultrasonic, X-ray and magnetic particle with their applications are introduced in section two and reviewed. In section three, several conventional MNDT techniques are reviewed together with their advantages and disadvantages. The application of AI in the conventional NDT techniques are described in section four and staged into three phases which are preprocessing, feature extraction and machine learning classification. Section five describes the existing techniques of AI in microwave NDT. Prospect of using artificial intelligence in microwave NDT is summarized in the conclusion section.

II. CONVENTIONAL NDT TECHNIQUES

A. THERMOGRAPHY NDT

A conventional thermography procedure is based on infrared (IR) radiation. The emitted radiation from the material under inspection is observed and captured using an infrared camera to represent the temperature distribution of the inspected material in a visible image [13]. Infrared thermography (IRT) is classified into passive and active thermography [14]. The passive IRT depends on the temperature variations between two mediums which are not in thermal equilibrium. While the active IRT depends on an external excitation source (e.g. flash lamp, ultrasonic waves or laser) for modifying the temperature of the inspected materials as shown in Figure 1. The defected area will generate a different temperature distribution from its neighbors which forms the shape of the defect. Thermography technique is considered as one of the most widespread in NDT due to the fast inspection, high imaging resolution and defect detection sensitivity. In NDT, the IRT techniques are usually limited to the active ones [15].

Pulsed thermography (PT) is used in active mode to inspect CFRP composites in [16]. In the first stage of the experiment,

the CFRP specimen is subjected to a pulsed-heating using two Balcar Xenon flash lamps whilst the specimen is observed by an IR camera. The heat will be transferred into the specimen and the temperature distribution will be decreased uniformly if the specimen is defect-free. In case of defect presence, it will affect the uniformity of the temperature distribution. This variation will be recorded using an IR camera for further processing. The camera is cooled during the inspection to 196.15 °C for mitigating the effects of the incoming temperature on the thermal detector. Two types of inspection are performed using PT;reflection and transmission. The reflection inspection is achieved by positioning the IR camera and excitation source in the same direction against the inspected specimen. On the other hand, the transmission inspection is performed when the inspected specimen is being between the IR camera and heating source. Both techniques perform an efficient inspection in locating defects of the inspected materials. However, a controlled environment of the inspection is needed such controlled ambient temperature and IR camera cooling. Moreover, a static position of IR camera is required to measure the amount of temperature on the inspected material at a particular time.

In the second stage of the experiment, ultrasonic waves are used as excitation source which named ultrasonic infrared thermography (UIT). The ultrasonic transducer excites the inspected specimen with a frequency of 20 kHz. The mechanical sound waves are propagated through the surface, if there is a defect on the surface, friction will be occurred by the crack. As a result, the friction will increase the temperature around the crack regions which will be recorded by IR camera. The advantage of this technique is that the crack itself will be the source of heating. Therefore, UIT successfully locates the CFRP defects which are more visible than the PT results. However, the suitable excitation source of IRT should be critically selected to avoid damaging the inspected materials. Actually, the excitation source changes the temperature of the medium under test. Therefore, the capability of the medium to be excited should be investigated first. Moreover, perfect control of the inspection environment is required to equally distribute the temperature on the inspected material. Therefore, the temperature is difficult to be controlled especially for inspecting the materials in service due to the variations of ambient temperature.

In addition, laser thermography (LT) in [17] is used to inspect glass laminated-reinforced epoxy (GLARE) which is a complex structure and widely used in aerospace applications. A matt black painting is applied on the surface of the inspected specimen to uniform the IR emissivity. A moving beam of the laser is focused with 1.5 mm spot for heating up the material under test. Moreover, the IR camera is used to acquire the temperature distribution on the inspected specimen. In case of defect presence such as delamination, a modification on the surface temperature will occur over the defected area. Standard division (SD) is used for post-processing of the defect representation. SD is applied on temperature distribution of the current laser spot and a reference area follows that point in the left side. The reference area has an elliptic shape which is positioned at 10 mm away from the laser spot with dimensions of 10 mm and 5 mm in x and y-axes respectively. Involving the reference area is because the position of the inner defect in composite materials does not correspond to the laser spot. The technique showed a very good detectability of the size of delamination. However, the small size of delamination is difficult to be evaluated because a small perturbation is induced over the reference area which is difficult to be observed. Moreover, the matt black painting is applied to the inspected specimen which is not practical to be used for inspecting in-service materials. In addition, critical positioning speed is required to avoid focusing the laser spot on the inspected specimen. This is possible to damage the coating paint. Finally, the reference area cannot be estimated when the laser spot in the left edge of the inspected specimen because the reference area is outside the inspected area.

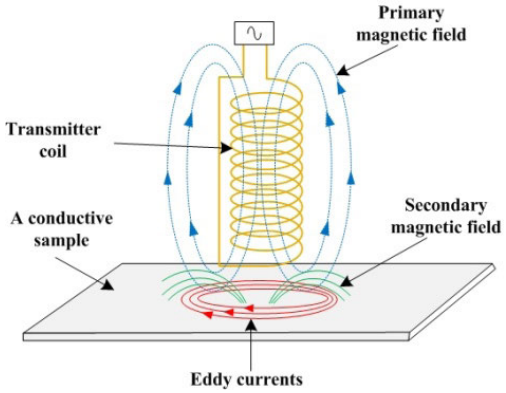

FIGURE 2. The principle of Eddy currents.

B. EDDY CURRENT NDT

Eddy current (EC) testing uses a transmitter coil to generate a primary magnetic field near the inspected specimen which is a conductive material [18]. Figure 2 illustrates the eddy currents which are formed on the conductive body opposite the coil. Eddy currents generate a secondary magnetic field which counteracts the primary magnetic field. In the case of defects presence such as discontinuity, the eddy currents become weak because the disruption of the crack to connect the currents which induce a weak secondary magnetic field against the primary magnetic field. Thus, the differences between the secondary magnetic field occur in the case of defected and nondefective regions.

EC testing is widely used in various applications. In carbon fiber reinforced polymer (CFRP) production, EC testing is used to detect fiber orientation and defects as well as accumulation of ripples and folds [19]. In term of aerospace applications, an EC technique is employed to detect the waviness in the aircraft structure [20]. Eddy current probe includes three coils were used to inspect the aircraft structure. All probes are placed above the sample to be inspected and the phase and amplitude of the output signal are measured to detect

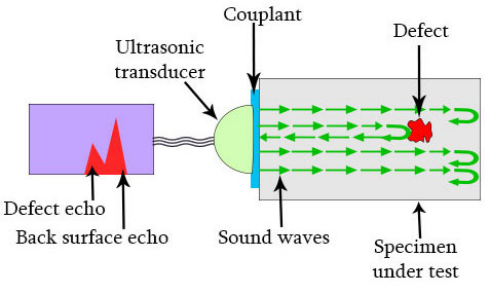

FIGURE 3. Typical ultrasonic pulse echo system.

the presence and location of the waviness of the inspected specimen.

In a different way, He *et al.* [21] examined eddy currents probes in various excitation modes to detect flaws in titanium alloy. In the first experiment, a small excitation coil is placed above the specimen under test to generate eddy currents to be detected by the high electromagnetic sensor. In this case, the excitation coil and electromagnetic sensor are moved along specimen under test to construct 2D spatial images based on phase and magnitude coefficients. The images are visually compared, and the finding shows that the phase image is the best to represent the flaws. In the second experiment, a large excitation coil is placed under the specimen under test. The coil covers whole titanium alloy and only the electromagnetic sensor is spatially moved to measure the changes of the yielded magnetic field. Similarly, to the first experiment, 2D spatial images are constructed based on phase and magnitude coefficients. In this case, the amplitude image shows a better representation of the titanium flaws. Therefore, the experiment conditions make large differences through choosing phase or amplitude in eddy currents imaging. Moreover, the scanning direction is another factor which gives an impact on the pixel intensity of eddy currents imaging which is clearly seen in the first experiment. In addition, the ripples of eddy current are clearly seen in the amplitude image of the second experiment which is undesirable noise because of the fixed position of the excitation coil. However, the optimal frequency is still manually selected, and the automated selection should be investigated. In most cases, the manual process is highly subjective and time-consuming.

Pulsed eddy current (PEC) is another technique of NDT which uses square wave voltage pulse to generate eddy currents in the conductive materials instead using the contentious sinusoidal signal. PEC is employed to inspect microcracks of aluminum alloys compared to the conventional EC in [22]. The study shows that the conventional EC can detect microcracks in the aluminum alloys, but PEC can provide more information about the crack depth due to the discrete frequency distribution which provides valuable information about the crack. However, eddy current based methods are restricted to be used in electrically conducting materials because of the lack of induced current in the dielectric materials which degrades the defects detection.

C. ULTRASONIC NDT

Figure 3 depicts the system of typical ultrasonic testing (UT) which employs a transducer to generate a beam of high-frequency sound waves that induced toward a specimen under test, travel through it and are reflected at back surface or defects [23]. The reflected wave is transformed into an electrical signal to be analyzed which will identify the presence and location of defects.

In NDT, ultrasonic is used for various inspection purposes such as crack detection, delaminations and corrosion detection. Various levels of intergranular corrosion of several stainless-steel pipes are studied in [24]. The study used a transmitter and receiver ultrasonic transducers to measure a longitudinal ultrasonic wave along the tube wall. The study shows that the ultrasonic non-linear coefficient is significantly increased with increasing corrosion level. As a result, ultrasonic NDT can detect the corrosion of steel pipe and estimate its level. However, the length of pipe highly influenced the non-linear coefficient because the longitudinal wave is degraded by the length of the inspected pipe.

Ultrasonic based on Lamb waves is another nondestructive technique which is popular to inspect plate-like structures. Lamb waves can propagate a long distance with low attenuation and are highly sensitive to small defects [25]. In case of defect presence in the inspected specimen, the defect will produce forward and backward scattering of waves. The scattering waves by the defect can be observed and evaluated for damage diagnosis. However, the reflected wave from the defect may overlap with that waves are reflected from the structure [26]. Moreover, most of Lamb waves are non-stationary in nature and needs effective time-frequency representation. The effective time-frequency representation is proposed in [25] possible to play a vital role in defect detection and localization. Among time-frequency techniques, continuous wavelet transform (CWT) is applied to process the Lamb waves signals to estimate a defect size and position on an aluminum plate. Four transducers are located on the corners of the aluminum specimen to receive the Lamb waves which are generated by an extra transducer on the plate center. The reflected waves from the defect edges are used to construct 4 ellipses to locate the defect. Thereafter, a circle is drawn based on the external tangent of all ellipses. The drawn circle is used to estimate the size of the circular defect. The technique provides near to the actual defect size and location. Moreover, the technique reduces the inspection time due to the induced Lamb waves cover the whole the inspected specimen in one time. However, the technique is limited to measure a circular defect shape.

The change in coupling material conditions is reflected in the inspection reliability due to the wave amplitude is affected by coupling variations. Equivalent Time Length (ETL) in [27] is employed to eliminate the coupling material effects on defect detection. The technique evaluated the bonding quality between CFRP and concrete using a pair of ultrasonic transducers. ETL is employed to measure the propagating

waves' energy with respect to its onset time which is small when the bonding is fitted well to the concrete. Therefore, the bonding weakness' level can be estimated due to the increasing ETL value. Thus, the defects such as air gaps between the concrete and CFRP can be detected. However, this technique is only suitable if the defect is away from the specimen edges because ETL value is affected by the position of the transducer when it is close to the boundary. Moreover, ultrasonic NDT based on couplant cannot be applied to an irregular surface [23]. It is limited in detecting defects of high anisotropy [28].

Laser ultrasonic (LUT) is a nondestructive technique has the advantage of being non-contact technique. In LUT inspection, a pulsed beam of the laser is distantly generated toward the surface of the inspected material [4]. A part of laser energy is absorbed and rapidly heat up the inspected region. The rising of temperature leads to expand the scanned region. As a result, the expansion of the scanned region propagates ultrasonic waves which interact with internal features and defects. The propagated waves can be observed on the surface using a contentious laser wave's detector for further processing.

LUT inspection in [6] is performed in transmission mode on additive manufactured components. The sample is combined from pre-alloyed AlSi12 powder was fabricated using selective laser melting which is popularly used in aerospace, automotive and medical engineering applications. The pulsed beam of the laser is induced on the inspected sample and the propagated wave is received using the contentious laser wave's detector. The laser detector is placed 50 mm away from the sample. The detector generates a time-varying analog signal which is proportional to the instantaneous surface displacement (e.g. 0.2 mm in both x and y-axis) on the inspected sample. The instantaneous displacement is converted into velocity using an analog processing module (APM). Thereafter, the analog signal is digitized at 8 bits using an analog-to-digital converter for further defect imaging. In the first stage, the acquired signals are analyzed using A-scan representation which provides the received amount of ultrasonic energy over time. A-scan is processed to produce B-scan representation which provides the traveling time of the sound waves at the scanned position. The maximum response is obtained between 1.6 and 2.3μs. Therefore, the surface representation will be obtained from the maximum amplitude of A-scan at that range. The technique provides several advantages which are a non-contact inspection to be used in an abnormal temperature environment, couplant is not needed, defect detection and imaging. However, the high intersection is seen between the defected and defect-free regions. This is because material porosity passes only the low-frequency and mitigates the high-frequency waves. Therefore, the power to resolve sharp defect's edges is low. As a result, accurate defect size is difficult to be measured. Moreover, safety hazards with high-power pulsed lasers should be considered and beam enclosures should be used to perform safe inspection [29].

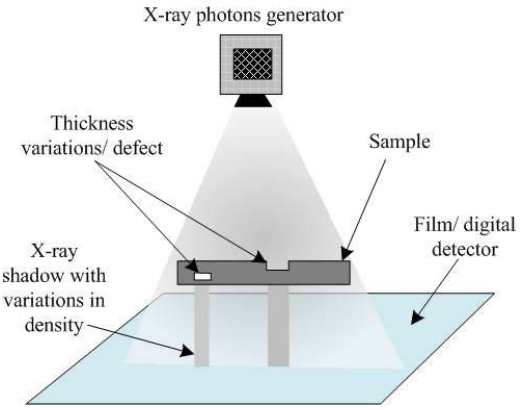

FIGURE 4. X-ray backscattering system.

D. X-RAY NDT

X-ray NDT based methods depend on the different levels of absorption of X-ray photons which pass through the inspected specimen [30]. Therefore, X-ray is sensitive enough to detect a change of the material thickness or density variations. Figure 4 shows the backscatter data of X-ray which contains quantitative information about variations in density, which is caused by changes in material properties or internal delaminations. Therefore, X-ray can be used to locate the internal non-homogeneities within the depth of the material [31].

These advantages of X-ray make it applicable in NDT for various purposes such as evaluation of aluminium alloy edged joints [32] and monitoring the quality of oil and gas pipes [33]. Moreover, the trend of using X-ray in digital form is an active topic among the researchers which allows the radiations of X-ray to be converted into digital data. This makes X-ray data is capable to be filtered and digitally processed. In [34], two sides digital X-ray NDT are used in pearl cultivation to check the presence of pearl nucleus without destroying the oyster shell. The study investigates the drawback of X-ray energy which is higher than that used by digital radiography. Therefore, optimization is needed to obtain high quality of the pearl image. The optimization is done by varying the voltage, current, and exposure time to acquire the optimal contrast to noise ratio (CNR) that can enhance the radiography image.

On the other hand, single side digital inspection technique is developed in [35] which used un-collimated X-ray radiation to inspect whole material. Twisted-slit collimator and digital array detector are used to construct a backscattering image. The specimen under test is placed on the 45° front of the X-ray tube and X-ray backscatter camera. The ambient noise such as undesirable radiations and structure noise is eliminated by subtracting the values of the digital array detector when the X-ray source and slit collimator are closed. Moreover, bad pixel correction is achieved using the in-house developed radiographic image quantitative analysis software to adjust grayscale pixels' values. Various materials are inspected such as aluminium sheets, honeycomb structured plate and an inhomogeneous component. The finding

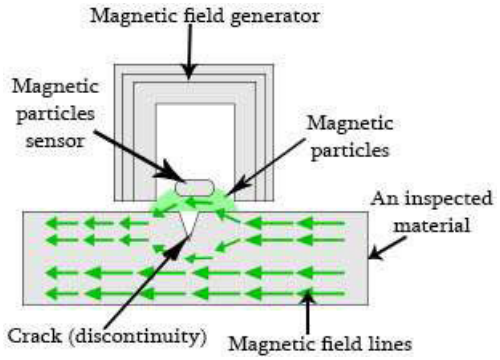

FIGURE 5. Illustration of magnetic particle principle.

shows an improvement of signal to noise ratio in the backscatter images. However, the heavy system's structure and a long time of acquiring an image are the main limitations of this technique.

Although its advantages, X-ray imaging is very challenging for large structures and harmful to human health as well as special protection is needed.

E. MAGNETIC PARTICLES NDT

Magnetic particles testing (MT) performs by magnetization of the inspected material first and the discontinuity of the inspected specimen generates leakage of magnetic flux [36]. Figure 5 illustrates the magnetic particles coil sensor which is near to the inspected surface can absorb magnetic particles and reveals the location, shape, size and severity of the discontinuity. MT is widely used in the heavy engineering, welding defects and aerospace applications to inspect the surface break, defects and discontinuity of the surfaces whether in production or in service. However, MT technique in NDT still suffers from reliability and sensitivity in detecting the surface cracks because it depends on the capability of the material to be magnetized and can only detect the defects in few millimeters below the surface [37]. The reliability and sensitivity of MT are investigated in [38] to detect cracks of welded components. The study shows that the technique is not capable to detect any defects with a length of less than 1.5 mm which is not reliable to detect a small size of cracks.

In [39], a magnetic conductive head is employed as a magnetic flux leakage sensor to increase the detection sensitivity to detect surface micro-crack in bearings. The sensor is placed in a parallel direction to the crack with small lift-off distance. The surface defect with 15 μm is detected and the weak magnetic flux leakage is picked up which is near to zero. The technique shows reliable inspection of the conductive materials and near surface crack. However, this technique is limited to conductive materials and surface cracks. The friction between the yoke's structure and bearing's surface may cause temperature increasing and damage the sensitive surfaces. In addition, the capability of this technique is only to classify the defected and defect-free bearings without further processing such defect localization and measurements.

.Sadr and Okhovat [40] presented the concept of the histogram for canceling the effects of a defect noise in computing background signal to inspect the pipeline's surface. The common techniques of defect detection based on the use of a simple threshold to distinguish between the defected and background regions which depend on the average of the acquired signal. Therefore, the approach uses particular regions around the peak histogram signal of the defect to calculate the average of the acquired signal because of the impact of the large difference between the defect and background values. Then, the threshold is applied to distinguish between the defected and background regions. As a result, the detection rate is increased compared to the typical average method. However, the technique is limited to the optimal threshold value to be selected.

Table 1 summarizes a comparison of various conventional NDT techniques. Thermography techniques perform a non-contact and remote inspection of complex structures such as CFRP and GLARE. Moreover, the excitation techniques hugely improve the sensitivity of thermography inspection in NDT. However, the selection of optimal excitation source is based on the capability of the inspected materials to be excited. Moreover, the selected excitation technique should consider the integrity of the inspected materials. Focusing high power of laser may damage the material under test. In addition, the controlled environment is the main issue faces thermography based techniques due to the difficulty of controlling the temperature in the real environment.

Eddy current based techniques show the high capability to detect the small surface's changes and microcracks evaluation. On the other hand, the main limitation of eddy current based techniques is the lack of the induced current in composite materials which leads to induce a weak electromagnetic field. Therefore, the weak electromagnetic field degrades the defects detection due to the low sensitivity. The ultrasonic NDT is capable to inspect conductive and non-conductive materials. Ultrasonic shows robust defect detection in the low porous materials and the small size of the inspected specimens. However, the sensitivity of ultrasonic is limited to the length of the inspected specimen which degrades the induced signals. Moreover, ultrasonic technique based on couplant material is not suitable for large structure inspection due to the coupling material should cover the whole inspected specimen. Among ultrasonic NDT techniques, laser ultrasonic is introduced to perform a non-contact and remote inspection which overcomes the couplant limitation. High porosity materials degrade the reliability of laser ultrasonic inspection. As regards to the Lamb waves technique, it performs fast inspection but it is limited to inspect plate-like structures.

X-ray NDT shows high sensitivity to layers' variations of the inspected materials whether conductive or non-conductive materials. The expert operator and safety procedures are critically needed.

The magnetic particles inspection shows robust surface defect detection. However, magnetic particles inspection is sensitive to the lift-off distance which is unreliable to inspect

TABLE 1. Comparison summary of various conventional NDT techniques.

Ref. No.	Technique	Concept of use	Advantages	Disadvantages
[16]	PT with flash lamps PT with ultrasonic	Defect representation of CFRP.	- Applicable to distantly perform one side inspection. - Defect detection and representation. - The defect itself will be the source of representation.	- The thermal detector should be cooled. - A controlled environment of the inspection is needed. - The capability of the inspected material to be heated should be investigated.
[17]	LT	Delamination detection and sizing of GLARE structure.	- A non-contact and remote inspection. - The reference area enhanced the defect detectability. - Identify defects with size as small as 10 mm.	- Small de-bounding size is difficult to be observed. - Applying matt black painting on the inspected specimen is not practical in the real inspection. - Critical positioning speed of the laser spot is required to avoid burning the coating paint.
[20]	EC	Waviness detection in the airplane structure	- One side inspection. - Identify a small waviness location.	- Cannot measure the size of waviness. - Limited to depth interrogation.
[21]	EC	Flaws detection and representation of titanium alloys.	- Low excitation frequency 70 kHz-100 kHz. - Sensitive enough to defect detection. - Defect's size can be seen.	- A pixel intensity value is affected by scanning direction. - Excitation coil should cover the whole specimen. - Poor spatial images. - Depends on which frequency point to be selected. - Two sides' inspection.
[22]	EC-PEC	Microcracks inspection of aluminum alloys.	- One side non-contacted inspection. - Microcracks detection. - Depth measurement of microcracks.	- Limited to deep crack depth. - To acquire accurate crack depth PEC must be integrated with conventional EC.
[24]	UT	Corrosion detection of stainless-steel pipes	- Corrosion level estimation.	- The sensitivity is limited to the length of the specimen under test. - Nonlinear of ultrasonic signal response is impacted by theory limitation. - Two sides contacted inspection.
[25]	UT	Defect detection, locating and sizing of aluminum plate.	- Lamb waves reduced the inspection time. - Estimating defect size and location.	- Inaccurate defect size and location. - Limited to measure a circular defect shape.
[27]	UT	Evaluation of bonding quality between CFRP and concrete	- Estimating bonding quality. - Robust to coupling effects. - Independent on wave amplitude.	- Unreliable to near edge defects. - It requires to first estimate onset time.
[6]	LUT	Defect representation of additive manufactured components.	- Non-contact inspection. - Defect detection and imaging. - It can be applied in the abnormal temperature environment.	- Two sides' inspection. - A valuable frequency is affected by material porosity leads to poor defects edges. - a pre-knowledge is needed to select the range of maximum amplitude of A-scan.
[34]	X-ray	Inspection of pearl nucleus.	- High sensitivity to layers' variations. - X-ray data capable to be filtered and digitally processed.	- Two sides' inspection. - Optimal contrast is required. - The expert operator is needed. - Safety hazards.
[35]	X-ray	Inspection of aluminum sheets, honeycomb structured plate and inhomogeneous component.	- Single side inspection. - High sensitivity to layers' variations.	- Heavy system's structure. - Longtime inspection. - The expert operator is needed. - Safety hazards.
[38]	MT	Crack detection of welded components.	- One side inspection. - Sensitive to normal surface cracks.	- It depends on the capability of the material to be magnetized. - Unreliable to detect a small size of cracks. - Limited to deep cracks.
[39]	MT	Detection of bearing crack	- One side inspection. - Sensitive to microsurface cracks. - Invariant to the small lift-off distance.	- Limited to the conductive materials and surface cracks. - Limited to defect localization and measurements. - Unsuitable for sensitive surfaces.
[40]	MT	Inspection of pipeline defects	- One side inspection. - Defect noise elimination. - Defect measurement and localization.	- The optimal value of threshold separation is needed.

the deep cracks. The lift-off distance increases when the defect far from the inspected surface which leads to the low sensor sensitivity. Additionally, magnetic particles technique highly depends on the capability of the materials to be magnetized to induce enough magnetic flux leakage in case of defect presence. Therefore, it can be only used to inspect the conductive materials.

Among the abovementioned techniques, ultrasonic provides safe inspection for both ferromagnetic and non-conductive materials as well as it can be used in contact and non-contact modes. In contrast, it suffers from the intensive data interpretation, and low penetration. Therefore, these limitations can be handled using microwave NDT inspection due to several attributes when applying Microwave NDT such as non-contact, interact with the inner structure, no need for coupling material, no need for complicated post signal processing, operator friendly and relatively inexpensive one-sided inspection [42].

III. CONVENTIONAL MICROWAVE NDT TECHNIQUES

In the past two decades, microwave NDT methods also have shown significant success in composite materials inspection. [44]–[46]. The composite materials become popular due to their stability, strength and lightweight characteristics, replacing metals in many applications such as aircraft, aerospace and automotive industries. This demands the popularity of microwave methods since microwave signals can penetrate composite materials and interact with their surface and inner structure.

Microwave NDT using microwave transmission line (MTL) sensor is presented in [41], [47]. In MTL technique, the inspected specimen acts as a conductive material of a microwave circuit. Any defect in the specimen will lead to change the material permittivity and will be reflected in the measurements of the signals' responds. These changes are used to detect the abnormality of the inspected specimen in term of defect location and size as well as the variation in the specimen layers.

The high capability of MTL to evaluate the materials' porosity employs it as an effective technique to evaluate the purity of honey to ensure the production quality [48]. Also, MTL is used in [47] to detect invisible pieces of stone and glass which were put in the vegetable salad. The proposed method measured the ratio of the real and imaginary parts of the transmitted signals to detect the foreign objects in the food. The detection is successfully achieved by comparing the objects and objects-free in the food and the variety in the values of the complex permittivity is shown which caused by foreign objects.

Todoroki *et al.* [41] construct a copper transmission line to detect the damage location on the carbon fiber reinforced polymer (CFRP) plate. The experiment used glass-fiber reinforced polymer (GFRP) as the insulator layer between the copper tape and the surface of the CFRP specimen as shown in Figure 6. Both conductors, copper tape and CFRP were connected by a coaxial cable at the end of the

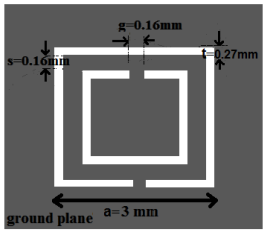

FIGURE 6. Exhibition of SRR sensor with pairs of concentric loops [43].

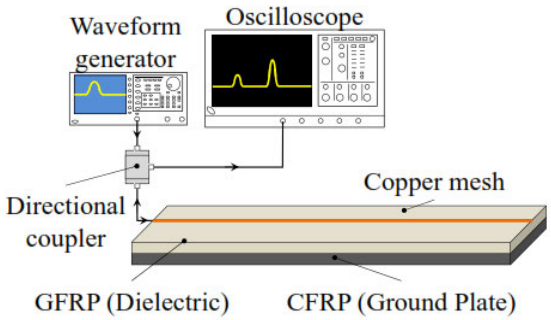

FIGURE 7. TDR connecting diagram based on the MTL sensor [41].

transmission line. The input signals propagate on the transmission line and any surface damage such as the changes of the distance between the copper tape and CFRP surface will change the impedance of transmission line at that location. Therefore, the signal will be reflected in the input terminal and the time differences between the induced and reflected signal is measured using Time Domain Reflectometry (TDR) to obtain the damage location. Approximate transmission velocity multiplied by the half of time difference is used to get the defect location. In this technique, the CFRP defect which is close to the transmission line is successfully detected and failed to detect the defect away from transmission line because the lack of capability of far away defects to change the impedance of transmission line. However, this technique can be used for near defect detection but using approximate transmission velocity near to the light speed may lead to a false defect location and exact measurement is needed. Practically, this technique is not suitable to inspect large structures because the copper strip and GFRP are needed to cover the inspected structure. In addition, MTL based techniques depend on the permittivity of the material to transfer microwave signals through it. MLT performance is degraded through low permittivity materials.

A split-ring resonator (SRR) is another microwave sensor which uses a small structure sensor includes pairs of concentric loops which are equivalent to LC resonant circuit etched in the lower dielectric substrate with splits them at opposite ends as demonstrated in Figure 7. The sensor requires a magnetic field for excitation where on the upper side of the substrate, a microstrip transmission line is used to feed the SRR sensor. In case of defect detection, the disturbance of the field around resonator leads to a shift in the frequency which indicates the detection of defects. The capability of

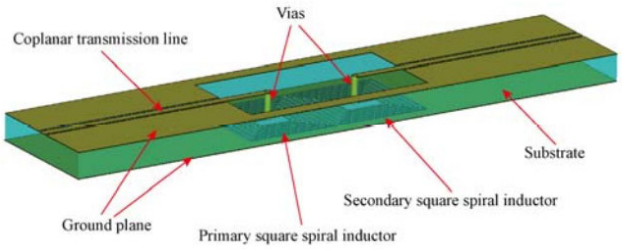

FIGURE 8. Schematic diagram of the CSI sensor [50].

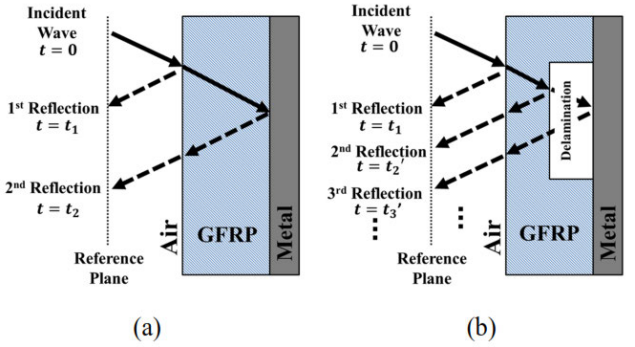

FIGURE 9. A diagram of the reflections from a metal-backed GFRP (a) without and (b) with delamination [52].

the single sensor is high to detect micro cracks on the metal surfaces [43], [49].

On the other hand, the SRR array is used to detect surface crack [51]. The proposed method used 9 SRRs together integrated with a microstrip line to inspect the aluminium specimen. A spatial image is constructed from the transmission coefficient by summation the values of the frequency amplitude which introduced a promising crack representation. However, the SRR technique depends on the capability of the transmitted signal to stimulate the SRR sensor. SRR technique has poor resolution inspecting low permittivity materials such as GFRP.

Figure 8 illustrates a couple spiral inductors (CSI) sensor. CSI consists of two spiral inductors which act as primary and secondary coils. The principle of this sensor based on the measurement of the transmitted energy from the secondary coil to the primary coil which is affected by the variations of the thickness of the inspected specimen. SCI is used to examine various kinds of CFRP defects such as buried holes, cracks, and delamination [53]. Li and Meng [50] used the SCI sensor to construct a spatial image of the CFRP defect. The sensor connected to the Vector Network Analyzer (VNA) is used to acquire the magnitude of transmission coefficient to construct a 2D image. However, the CSI method is not suitable for geometrical measurements of the defect due to the diffraction at the defect's edge which extends to the defect-free area.

A significant amount of research and development has taken place using different open-ended rectangular waveguide (OERW) microwave probes for various types of examination such as delamination evaluation in the layered-

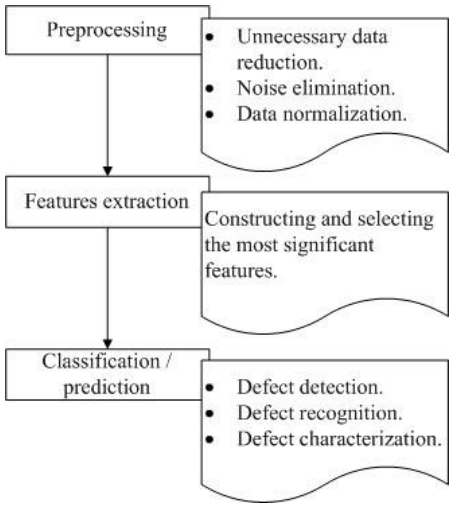

FIGURE 10. Common stages of intelligent NDT.

dielectric slab, thickness variation in a stratified composite and defect sizing and detection of coated metal. The shift in the resonant frequency, magnitude and phase of the microwave signal is used to identify and image the defects. Akbar *et al.* [52] proposed a time domain technique using OERW to detect the delamination in metal-backed dielectric coatings. The proposed approach assumes that there are two reflected signals will be obtained from the defect-free sample at different times. The first reflection is from the coating surface (e.g. GFRP) which comes early because of the coating proximity to the waveguide as shown in Figure 9 (a). The second reflection is from the back metal surface which comes late because of the distance from the waveguide. The reflected signals are denoted as t_1 and t_2 respectively. In the case of delamination, as shown in Figure 9 (b), there are three reflected signals will be obtained which are from the coating, delamination and back metal at three different times denoted as $t_{1'}$, $t_{2'}$ and $t_{3'}$ respectively where $t_{2'}$ comes between $t_{1'}$ and $t_{3'}$. In the delamination presence, the magnitude of $t_{3'}$ will be reduced compared to t_2 reflection from the defect-free sample. This reduction occurred because the impact of $t_{2'}$ on $t_{3'}$ which means that the signal does not fully reflect from the back metal and there are some reflections occurred before. Therefore, any drop in the magnitude of $t_{3'}$ compared to t_2 can provide information about thickness variations and delamination detection. The results have shown the ability of this technique to detect delamination of depth as low as 1 mm.

Guorong *et al.* [54] used OERW to detect a surface crack on the substrate under a thermal barrier coating (TBC). The investigation studied the best defect detection and representation based on the phase and magnitude of the reflection coefficient under various thicknesses of the coating. The difference of amplitude and phase between the defected sample and non-defected sample is used to plot 2-D spatial images. The result shows that the amplitude image is more sensitive for defect detection than the phase image. However, both phase and amplitude fail to accurately image the exact geometric size and location depth of the defects.

As a near field technique, there are several factors influence the defect detection capability such as frequency point and stand-off distance which is the distance between the probe and the specimen to be inspected. Similarly to the previous method, the differences of amplitude and phase of the reflection coefficient between the defected area and non-defected area in [5] are used to investigate appropriate OERW stand-off distance and frequency point to represent the defect undercoating. The defect representation using the amplitude differences with 1 mm stand-off distance is the optimal distance to detect the defect undercoating compared to 3 mm and 5 mm distances in this experiment. The study shows that among the selected frequency points which are 18, 22, 24, and 26 GHz, there is an appropriate frequency point (e.g. 24 GHz) which provides a better defect representation at 1 mm stand-off distance. Therefore, selecting optimal stand-off distance and frequency point is required in each experimental setup due to the variations of the coating thickness and the experimental conditions.

Firdaus *et al.* [55] used a correlation approach of the reflection coefficient at various stand-off distances for each inspected point. The proposed method eliminates the process of selecting the optimal frequency points for both phase and magnitude imaging technique and shows a promising result for various stand-off distance.

A microwave-based technique for steel pipeline inspection is proposed in [56]. The technique aims to inspect curvature surfaces (hyperbola shape) in far standoff distance (40 mm). Several of microwaves OERWs with different bands are used to acquire the best spatial image representation. Singular value decomposition (SVD) is used to reduce the clutter of the insulation layer as well as to distinguish between the insulation layer and the pipe layer. SVD decomposes the signal into singular values and singular vectors. The first singular vector which is associated with a given singular value represents the insulation subspace and the rest of singular values are considered as subspace distortion. Thus the insulation subspace can be separated. However, the output image still suffers poor resolution due to the high standoff-distance and the hyperbola shape of the pipeline.

Therefore, the rang-Doppler algorithm (RDA) is used to refocus the blurred data of SVD and obtain a high-resolution image. RDA involves three stages which are range compression, rang cell migration and azimuth or cross-range focusing. The range compression stage aims to convert the raw data from the spatial domain into the frequency domain using a discrete Fourier transform (DFT). The range cell migration stage aims to correct the migration of the data which is acquired by the curvature movement of the sensor as a result hyperbola shape. The last stage is cross-range (azimuth) focusing; this aims to focus on the target point which is buried under the insulation layer. Finally, inverse DFT is applied to construct a high-resolution image in the time domain and the defects are clearly seen.

Table 2 summarizes a comparison of various conventional MNDT techniques. The MTL sensor shows good performance for detecting near-surface defects and used to evaluate the properties of the material. However, MTL is not reliable to detect the defects in non-conductive materials because its performance is degraded due to the low permittivity of the non-conductive materials. On the other hand, the SRR sensor achieves a reliable detection of the near-surface micro-crakes. However, the performance of the SRR sensor highly depends on the capability of the transmitted signal through the inspected material to stimulate the SRR sensor. This degrades the sensitivity of SRR in the case of low permittivity of the inspected materials. The CSI inspection provides a good detection of various types of defects but it makes the evaluation of the detected defects very complex. This is because the diffraction at the defects' edge extends to the defect-free area which introduces a blurred spatial image. Therefore, it is difficult to measure the accurate defect size because of the high intersection between the defected and defect-free regions. Among microwave sensors, OERW provides robust signal interaction with multiple layers of structures. However, the performance of OERW is degraded because stand-off distance variations and optimal frequency point to be selected. Therefore, a pre-knowledge of those variables is needed to achieve the best imaging quality and reliable inspection.

It can be noted that most of the microwave inspections suffer from the low sensitivity of defect detection and unreliable defect evaluation. In term of best sensor sensitivity due to the low signal penetration, hybridizing the signal processing techniques and artificial intelligence (AI) models is possible to improve the sensitivity of the sensor. Various attempts are introduced in section IV demonstrate the capability of the signal processing and AI to improve the conventional NDT sensitivity. Also, this will be reflected in the microwave NDT (MNDT) technique performance due to the lack of studies to integrate the signal processing and AI in MNDT. The data complexity is presented due to the stand-off distance variations and optimal frequency point selection which lead to unreliable defect evaluation (e.g. defect location, size and depth). Section V introduces various possible AI approaches to overcome these challenges.

IV. ARTIFICIAL INTELLIGENCE APPLICATIONS IN CONVENTIONAL NDT

As described in Section II, the conventional NDT techniques still face several challenges due to the automation complexity [57], poor quality of the spatial image and blurred defect shape, extensive data interpretation as well as penetration limitation which degrade the inspection reliability. Recently, the development of NDT automation with high reliability has emerged as an active research area [58] because of the needs of avoiding the dependence on the skills and experience of the operators [57]. Therefore, signal processing with intelligent classifier can provide reliable and fast inspection [59] which could increase the sensibility of defect detection and automate the monitoring procedure [60]. The nonlinearity of inspection data is another reason to use AI due to its capability

TABLE 2. Comparison summary of the conventional MNDT techniques.

Ref. No.	Technique	Concept of use	Advantages	Disadvantages
[41]	MTL	Defect detection and localization of CFRP.	- Sensitive to near surface defects. - One side inspection.	- Limited to deep defects. - Unsuitable for irregular surfaces. - An insulator layer is needed. - Approximate transmission velocity near to the light speed may lead to false defect location. - It is suitable only for conductive materials.
[51]	SRR	Defect inspection of the aluminium specimen and spatial image representation.	- High sensitivity to detect near-surface microcracks.	- Depends on external magnetic circuit for excitation. - Poor quality of the spatial image.
[50]	SCI	Construct a spatial image of CFRP defects.	- Detection of buried holes, cracks, and delamination defects. - One side inspection.	- Blurred defect shape. - Unsuitable for geometrical measurements of defects.
[52]	OERW	Delamination detection in GFRP using time domain reflectometry.	- One side inspection. - Non-contacted technique. - Underneath defect detection.	- Pre-knowledge of frequency point is needed. - Free defects sample reference is needed.
[54]	OERW	Surface crack detection of the substrate under TBC and spatial image representation.	- One side inspection. - Non-contacted technique. - Underneath defect detection.	- Blurred defects edge due to data complexity. - False defect detection.
[55]	OERW	Turbine blades defect detection and representation.	- Defect detection and localization. - Able to measure defect depth. - Invariant to the near stand-off distance. - No needs to pre-knowledge of optimum frequency.	- Free defects sample reference is needed. - Poor quality of the spatial image.
[56]	OERW	Curvature pipeline inspection and spatial image representation.	- Far standoff distance. - High-resolution image.	- Free defects sample reference is needed. - Mathematical computations intensively used which is time-consuming.

to solve the complexity of the acquired data by nonlinear classification [61].

Commonly, intelligent NDT passes through three stages. VI illustrates common stages of the intelligent NDT. The first stage is a preprocessing phase which aims to eliminate the noise and normalize the acquired signals. The preprocessing stage in NDT employs signal processing techniques to reduce the noise effects and eliminate unnecessary data. The second stage is the features extraction and selection which aims to extract and select the most significant features for defects evaluation. Finally, the classification or prediction stage aims to classify and recognize the defects as well as to estimate the defects' characteristics. In this section, the stages of intelligent NDT and various techniques involved in each stage are reviewed.

A. PREPROCESSING TECHNIQUES

Tiwari *et al.* [62] performed an analysis of ultrasonic NDT on wind turbine blades. The study aims to investigate three types of de-noising algorithms which are the cross-correlation (CCR), Hilbert-Huang transforms (HHT) and discrete wavelet transform (DWT) methods. The experiment used two contact transducers in the inspection process as a transmitter and receiver. The first de-noising algorithm called cross-correlation technique is based on the similarity measurement between two signals. The cross-correlation value will be a maximum when the time delay is zero [63]. Therefore, this technique can be used for comparing the time delay of the acquired signal with the reference signal. The time delay will be higher in case of the defect presence. In case of the occurrence noise, the variation of the time delay will be eliminated for the similar waveforms because it is considered as a noise delaying. In the experiment, the A-scan signal is acquired along the scanning distance and the cross-correlation coefficient is calculated based on the reference signal of the defect-free to illustrate the variation of time of flight (ToF). Finally, a simple threshold is applied which successfully displayed the peaks of the defected areas. Cross-correlation technique is the easiest method in signal processing despite having a lot of computation iterations. This technique depends on the shape of the waveform such as peaks and fronts of wave pulses to measure the time shifting for the similar waves. Therefore, it may fail in case of strong waveform deformation due to the high disruption which leads to change the exhibition of the waveform. Moreover, it cannot be used to measure the accurate defect size when the noise is part of defects because the noise can be only eliminated from the provided sample which

is defect-free. In addition, this technique needs defect-free reference specimen during the inspection process and it is not practical in the real applications due to the manufacturing variations. Another technique proposed by [64] used defect-free regions in the same inspected specimen but still, those regions are unpredictable in case of the coating.

In the second part of the experiment, Hilbert Haung transform (HHT) is examined for noise suppression. HHT an empirically based approach is a time-frequency analysis which is used for nonlinear and non-stationary processes representation [65]. The signals can be decomposed using HHT into several narrow-banded signals which varies in frequency and amplitude over time. Two stages are involved in HHT which are empirical mode decomposition (EMD) and Hilbert transform (HT).

EMD as described in [66] is the essential part of HHT which aims to identify the proper time scale which can describe the physical characteristics of the input signal. Therefore, EMD does not convert the signal from the time domain to another domain but it produces a nearly orthogonal basis for the input signal without leaving its domain. The output of EMD is several intrinsic modes of the signal called intrinsic mode functions (IMFs) which are the frequency distribution over time. In this stage, the input signal is smoothly enveloped based on the maxima and minima of peak signal to construct upper and lower envelopes in the time domain. Then, the mean value is calculated which produces zero difference between upper and lower envelops at each time point. To produce the first IMF, at each point in the time domain, the mean value at that point is subtracted from the original signal value. This process will be repeated several times by utilizing the produced IMF as input to generate the next IMF until the number of extrema and zero-crossing remain the same. Each IMF contains varying frequency and amplitude from the others and can be used to serve HT. In some enveloping cases of the signal extrema (e.g. similar to single digital waveform), there are many contiguous points in the extrema have similar values with different time points. In this case, choosing a single enveloping point in EMD suffers from that at which time point of them to be selected. Therefore, various shapes of IMF can be produced and give impacts on the next IMFs behavior.

Basically, the first IMF contains the highest frequency oscillations which are decreased at the last IMF. Therefore, the selection of an approbate IMF to be passed to HT analysis is needed which is done based on the signal amplitudes that can keep important details of the inspected specimen. Mostly, the required information is kept in the first few modes. However, the time of generating the first IMF is more than the required time to generate the last IMF because the signal peaks to be enveloped at the first IMF is larger than the last one. Therefore, the processing time can be reduced by overcoming the over-enveloping [67] as well as if the n^{th} IMF can be predictable from the original signal. This is still challenging because generating the n^{th} IMF basically depends on its previous IMF.

The last stage of HHT is a Hilbert transform which aims to interpret the signal with varying frequency and amplitude. The input signal such as IMF_n is converted into the frequency domain and 90° phase shifting is applied at each frequency component to be converted again into time domain [66]. This step aims to find the instantaneous frequency and amplitude representation. Applying HT provides many characteristics of the processing signal [68]. The first attribute is that the input signal and its HT have the same amplitude density spectrum. Secondly, the input signal and its HT have the same autocorrelation function which indicates they are correlated to each other. The third attribution is that the input signal and its HT are mutually orthogonal, thus their integral equals zero. Finally, applying HT of the input signal will produce the negative original signal where it is capable to be inverted. However, HT is limited to be applied for narrow-band signals because it uses a sinusoid narrow-band [69]. Therefore, it is not applicable to process broadband signal which is a common kind of the signal in the real applications.

For defect detection in the experiment, A-scan signal of the defect and defect-free regions are acquired and passed to empirical mode decomposition (EMD) stage. In the experiment, HT is applied on the first four IMFs of the defect and defect-free signals and only the first two IMFs are used for defect analysis. The two selected IMFs have a higher amplitude as compared to the rest of IMFs as well as less noise and dispersion. Therefore, the time-variant frequency and instantaneous amplitude of the first two IMFs are computed using HT for both defect and defect-free regions. In defect detection, the instantaneous amplitude of the defect and defect-free regions is different which represents the first attribution of the defect detection. In addition, the study shows that the time delay is correlated to the defect size because it is increased by increasing the defect size and vice versa. Thus, HHT can be used for defect detection. However, the selection of an IMF to be passed to HT is depended on which signal to be analyzed because there are several IMFs without prior knowledge about the optimal one. Moreover, HHT is restricted to be used in time domain signals processing because it does not convert the signal to another domain. In addition, the time shifting is used to detect the defects which came after the defect-free. Therefore, any variation in the time during the inspection process of the defect and defect-free samples will lead to false defect detection.

In the final stage of the experiment, discrete wavelet transform (DWT) is used for noise reduction which is a powerful technique for signal representation in the time-frequency domain. Basically, wavelet transform analyzes an input signal as a sum of wavelet functions called ''wavelets'' in different locations and scales [70]. Haar and Daubechies wavelets are the common types of wavelet transformation functions. The main difference between them is that Daubechies wavelet uses a non-linear phase response compared to the linear phase response of Haar wavelet [71]. Moreover, Daubechies wavelet involves a large number of vanishing moments compared to the Haar wavelet which its interval between 0 and

TABLE 3. Comparison summary of the preprocessing techniques.

Ref. No.	Technique	Concept of use	Advantages	Disadvantages
[62]	CCR	Investigating the efficiency of de-noising algorithms with the ultrasonic inspection.	- Easy to implement. - Noise elimination based on waveforms' similarity between two signals. - Time delay can be used as a feature for further -post-processing.	- A reference signal of the defect-free sample is needed. - The optimal value of threshold separation is required. - A lot of computation iterations. - The technique may fail in case of strong waveform deformation. - Inaccurate defect's size when the noise is part of the defect.
	HHT		- Nonlinear and non-stationary noise suppression is based on EMD. - Various features can be extracted such as instantaneous amplitude and time shifting. - It can detect and measure the defect size based on the given features.	- A reference signal of the defect-free sample is needed. - Not suitable to process broadband signals. - EMD enveloping process suffers from the optimal time point of extrema to be selected. - Prior knowledge is required about the optimal IMF to be selected. - It is restricted to be used in the time domain.
	DWT		- A powerful technique for signal analysis in the time-frequency domain. - It provides approximate and details characteristics. - In NDT, Haar wavelet sensitive for sudden changes such as defect monitoring. - Data compression and reconstruction. - In hard thresholding, the optimal value is not required.	- A pre-knowledge of a certain level of wavelet decomposition is needed. - In soft thresholding, the optimal value is required. - An approximate signal does not fully represent the original signal. - Selecting an optimal wavelet function is required.

1 unit. Therefore, Daubechies uses few values to represent the input signal because of its vanishing moments slightly longer than Haar wavelet. However, the wavelet capability to represent an input signal depends on the number of vanishing moments because the high number of vanishing moments can represent complex high degree polynomials [72]. On the other hand, the Haar function is discontinuous and not differentiable because it is similar to a square shape of the digital signal. This property of Haar wavelet can be an advantage to analyze signals with sudden changes such as defect monitoring [73]. The wavelet function to be selected is moved along the input signal with a particular shifting period. In this stage, the input signal is decomposed through high and low pass filters which perform averages and differences respectively. The output of low pass filter is an approximate signal which is down-sampled by 2 while the output of the high pass filter is the details coefficients and also down-sampled by 2 which can be used to inverse back the approximated signal to its organic [74]. This process can be repeated several times to produce several decomposition levels using the approximate signal as input for DWT. Therefore, several advantages are provided using DWT such as higher data compression and reconstruction [75] as well as de-noising preprocessing.

In the noise reduction, the input signal is decomposed into a certain level with keeping its details coefficients, followed by hard or soft thresholding. The hard thresholding makes all the details coefficients equals zero while the soft thresholding only makes particular coefficients equals zero which are lower than a certain value. Finally, the signal is reconstructed using inverse discrete wavelet transform (IDWT) by involving approximation coefficients and the modified details coefficients. The reconstructed signal is less deformation than the original one but it actually does not form the original signal [76] because the occurred changes by thresholding in the details coefficients. In the experiment, A-scan signal is decomposed into several levels using DWT and it is found that the signal at level 8 contains the minimal noise and the defects are clearly seen. However, a pre-knowledge of the certain level of wavelet decomposition and adequate thresholding value is required instead of analysis all levels of wavelet decomposition which is time-consuming. Therefore, the automation to select the optimal values of those coefficients is a real challenge in DWT based techniques [77].

Table 3 illustrates a comparison of various preprocessing techniques. CCR is easy to be implemented in NDT for signal de-noising purpose. This is applicable if a reference of the pure signal is available to eliminate the waveforms variations between the acquired and reference signals. Moreover, CCR can provide time delay variations for defect detection. Therefore, it can be used as a feature in post processing for defect evaluation. In the case of HHT, the technique is restricted to be used in the time domain for nonlinear and non-stationary noise suppression of the narrowband signals. Beside de-noising function, HHT provides various features such as the instantaneous amplitude and time shifting which can be used for defect evaluation too. However, prior knowledge is required for the optimal IMF to be selected.

Therefore, putting the optimal IMF selection as an optimization problem is possible if the optimal solution is available. Similarly, in the case of DWT, the selection of a certain level of wavelet decomposition which is noiseless should be optimized. Among the abovementioned techniques, DWT is a powerful technique for signal analysis due to its capability to analyze the signal in the time-frequency domain. Moreover, the data compression provided by DWT can be employed to handle the data storage issue in case of a large structure inspection. In addition, DWT can provide approximate and details coefficients as features for further post-processing of defect evaluation.

B. FEATURES EXTRACTION

Features extraction and selection are important factors for classification related issues. The appropriate set of features can improve the classification decision and will be easily processed by the classifier [78]. Therefore, the quality of features is more important than their quantity. In NDT, Liu *et al.* [64] used three signal based coefficients to construct a feature vector. The features are used to recognize various defects' shapes of aluminum specimens including arc slots and inclined cracks. The features' vector is a combination of the amplitude of eddy current which is the difference between the maximum peak value and the corresponding point in the reference line. The second coefficient is the area between the signal curve and the reference line. The last feature is the width which is the number of points between the starting point and the ending point of the defect's signal. The maximum classification accuracy of 98.90% is achieved using an optimized support vector machine (SVM) classifier when the large training set is used which is 173 samples. In addition, the selected features achieved an acceptable recognition rate in the case of small training sample (i.e. 19 samples) which is 82.87%. The technique provides an effective small feature vector to automate the recognition of various defect shapes. However, a clear signal curve of the defected area is used to construct the features' vector. Therefore, the peak value, area and width of the signal's curve are easily computed. However, it is difficult to compute those coefficients when the noise is part of the defect due to the high disruption of the signal's curve or waveform. A robust de-noising preprocessing is needed to clarify the exhibition of the waveform in order to make this technique effective. In the matter of the reference line, it connects the front and end of the signal wave. The difference in the amplitudes of the front and end of the signal wave yields italic reference line. In the case of presence several peaks in the same maximum value, the differences between the similar peaks with their corresponding points on the reference line will produce different values. Therefore, there is no clear decision at which point the feature will be calculated.

In other technique [79], several statistical parameters are used to represent the features of the ultrasonic signal which are mean value, root means square value, standard deviation and absolute value as represented by Equations 1, 2, 3 and 4 respectively.

$$\text{Mean value: } AVG = \frac{1}{N}\sum_{i=1}^{N} x_i \tag{1}$$

$$\text{Root means square value: } EFC = \sqrt{\frac{1}{N}\sum_{i=1}^{N} x_i^2} \tag{2}$$

$$\text{Standard deviation: } STD = \sqrt{\frac{1}{N-1}\sum_{i=1}^{N} (x_i - AVG)^2} \tag{3}$$

$$\text{Absolute value: } ABS = \sum_{i=1}^{N} |x_i| \tag{4}$$

where N is the number of the acquired points and x is the echo amplitude of the back wall echo at a certain point i.

A-scan signal is obtained from steel and coarse-grained metallic material and preprocessed using DWT. A hard threshold is applied to the details coefficients at each decomposed level to improve the signal-to-noise ratio. The features are computed from the echo amplitude of the ultrasonic signal. The technique proposed that the signal which contains only the back-wall echo has a smaller average value than the signals obtained from flaws or welding regions due to the variations of echos number. The acquired signals are mapped based on the computed features to three classes which are a place without flaw, a place with a flaw and in the center of the weld. Then, the features are classified using SVM classifier and 100% of classification accuracy is achieved by the feature of root means square value. Moreover, the statistical parameters with different strategies are introduced in [80] to form the feature vector of the ultrasonic signal. The classification is achieved using SVM and ANN to recognize various defects (i.e. void, delamination and debonding) of CFRP and more than 98% of recognition rate is achieved. However, statistic features especially average based features aim to reduce the higher echos and must be considered as a loss of valuable information in case of data representation.

A comparison of the feature extraction techniques is summarized in Table 4. All the described techniques show high performance in term of defects recognition and classification. In [64] only three features are used to automate the defects recognition. The low features' dimensionality shows a robust recognition rate with a small training sample set. Therefore, the difficulty of collecting the training sample of NDT application is considered. On the other hand, the statistical features in [79], [80], the higher accuracy is achieved in [79] by hybridizing the signal processing (e.g. DWT) and machine learning (e.g. SVM). The statistical features acquired after signal processing and hugely improved the classifier performance with 100% of classification accuracy. Therefore, the signal preprocessing is needed to improve the features' quality to be reflected in the classifier performance.

C. NDT MACHINE LEARNING BASED TECHNIQUES

1) ARTIFICIAL NEURAL NETWORK (ANN)

ANN is data processing pattern which simulates a biological brain through simple computational elements known as neurons (nodes). Basically, ANN is limited to three layers which

TABLE 4. Comparison summary of the feature extraction techniques.

Ref. No.	Technique	Concept of use	Advantages	Disadvantages
[64]	EC based features and SVM classifier	Recognizing various defects' shapes of aluminum specimens	- Automation of the NDT process. - The maximum recognition rate of 98.90% is achieved using 173 samples as the training set. - Acceptable result of recognition rate is achieved using a small training set which is 82.87% with 19 samples.	- It is difficult to compute the features with high disruption of the signal's waveform. - A robust de-noising preprocessing is needed to clarify the exhibition of the waveform. - In the case of presence several peaks in the same maximum value, there is no clear decision at which point the feature will be calculated.
[79]	Statistical parameters as features of UT signal with DWT and SVM classifier	Classifying metallic materials into three classes which are a place without flaw, a place with a flaw and in the center of the weld.	- Automation of the NDT process for defect detection and recognition. - 100% of classification accuracy is achieved using root means square value.	- In NDT imaging, the use of statistical features leads to loss of valuable information in case of defects' representation. - The techniques do not provide any information about defects' size, depth and location.
[80]	Statistical parameters as features of UT with SVM and ANN classifiers	Classifying CFRP specimens into three classes which are void, delamination and debonding.	- Automation of the NDT process for defect recognition. - High performance of recognition rate is achieved with a complex structure which is 98%.	

are input layer, hidden layer and output layer. Several neurons involved in the hidden layer which is fed by the inputs' values that are weighted and summed to be decided whether the neuron should be activated or not for producing the output signal [81]. The artificial neurons work in unison which has a natural behavior to build investigational knowledge to be used for classification and estimation purposes based on the learning by actual example. This advantage of ANN as an AI model can be employed in NDT to recognize and estimate harmful defects before causing the system failure as well as improve the safety criteria.

ANN is used in [82] to estimate the strength of concrete underwater and provide efficient maintenance process of construction integrity. The training process used the real compressive strength values are labeled with corresponding values of ultrasonic velocities and rebound hardness which represents the pattern features. The training set used 14 out of 20 samples and the rest of the sample used for experimental verification. The verification result showed that 98% of accuracy is achieved which provides a robust estimation of concrete strength. However, a large sample is needed to improve the estimation reliability [83] because a small size of the verification sample in some cases leads to the accuracy bias.

The automation of defect detection and improving sensor sensibility are other challenges that are faced by conventional NDT techniques. These challenges are due to the data complexity produced by sensors which require a long time for processing and intensive computations. An intelligent model such as ANN makes it possible to develop real-time NDT applications and improve defect sensibility. Automatic defect recognition is developed in [60] based on ultrasonic oscillogram and DWT coefficients. Three defects to be recognized using ANN which are porosity, lack of fusion, and tungsten inclusion, as well as the defect-free regions, are considered. A-scan signals are acquired from the inspected stainless steel specimen and eight features are extracted from DWT detail coefficients at each known defect position namely mean, variance, maximum amplitude, minimum amplitude, maximum energy sample, average frequency, minimum frequency and half frequency point. A database from 240 sets is produced to train and test ANN. A pre-test involves 12 sets of each class is achieved first. The goal of the pre-test is to acquire the weight values of ANN at a lesser epoch. The acquired weights are applied to another untrained network has the same previous ANN structure which is detailed in the original article. The pre-test aims to generate adjusted ANN without long training process or massive training set and capable to perform reliable defect recognition. The rest of dataset is used to examine the untrained ANN and 94% of recognition rate is achieved. The integration between signal processing technique (DWT) and artificial model (ANN) produces reliable automatic NDT which can achieve a human expert's function. Therefore, the proposed method shows the suitability for the development of a decision support system for nondestructive evaluation. However, this technique is limited for defect classification based on the whole specimen under test. It is not capable of defect localization because it classifies the specimen into various classes of the defects. This means the accurate location affected by the defected regions is merged together with adjacent locations. In addition, the appropriate weight values of ANN are needed to generalize the defects classification which depends on the appropriate set of features that can improve the classification decision.

2) DEEP NEURAL NETWORK (DNN)

Recently, deep learning achieved astonishing success in various areas, especially in image processing. DNN is a

hierarchical structure of ANN which involves nonlinear multiple layers that aim to create an efficient link between the input and output layers by adjusting network weight during the training process [84]. Increasing the hidden layers will increase the network capability to transform the input data in more complex manners to its target output through a training process. In the case of the composed materials inspection, the inspection produces a complex backscattering due to the presence of the hidden defect. The complex backscattering makes difficult to distinguish between the defect and defect-free regions. Therefore, DNN is well suited to process the huge data of the complex backscattered signals to find out the features of the hidden defects to be distinguished from defect-free regions as well as to recognize various kinds of defects [81]. This assists to improve NDT performance and provide a reliable inspection.

DNN-NDT in [58] is performed to detect the presence of various kinds of defects such as drilled holes and slits with different depths. The inspection is based on the ultrasonic images. Massive training sample with 6849 images is used to train the network to split the sample into the defect and defect-free sets. The study shows that the deep learning network outperformed the ANN performance. On the other hand, various DNN-based techniques are well reviewed in [81] which are used to inspect the materials degradation. The review shows that DNN produces encouraging results for detecting materials degradation whether image-based inspection or signal based inspection. However, deep learning network still suffers from massive training sample which is needed to achieve high-performance accuracy. Practically, this massive sample in NDT is difficult to be acquired for the same sample under the inspection. Moreover, a large number of hidden layers and learnable coefficients are needed for accurate classification which makes DNN suffers from overfitting without regularization to integrate this massive structure of DNN [57]. In addition, in case of high noise of ultrasonic NDT, DNN gives the poor performance of defect detection compared to the conventional neural network [85].

3) SUPPORT VECTOR MACHINES (SVMS)

SVM is a machine learning technique that aims to analyze data for classification and estimation purposes. During the training process, there are two input groups which are v and c where v is an n-dimensional vector contains set of properties of an object, and c is a label or a classification of the features vector. The classification and estimation processes are achieved by providing only the features vector c without its label which will be classified or estimated [86].

As a part of AI techniques, SVM can provide reliable and fast recognition NDT of defects which is an essential task for structural integrity and health monitoring. SVM aims to decrease the upper bound of the generalization error, which enables the SVM to provide better generalization capability even when dealing with unseen data. SVM is intensively used in NDT because of its advantages such as performing reliable classification and handling high-dimensionality features as well as the perfect generalization capability. SVM is used not only for defect detection but also for various defects recognition. The capability of SVM to distinguish between two classes is high due to its advantage as a binary classifier [87] which performs a robust classification between two classes (e.g. 0 for defect-free and 1 for the defected region). The demands of online NDT to obtain satisfactory accuracy with low time cost are required. An intelligent system is introduced in [64] to realize an online automatic NDT and recognize various defects shapes. The proposed system consists of eddy current sensor, wavelet packet analysis (WPA) for denoising processing, defects feature extraction and SVM. The system is used to identify common defects (i.e. arc slots and inclined cracks) of aluminium alloys and performance accuracy of 98.90% is achieved based on three features which are peak value, area and width of the defect signals. As shown in the recognition accuracy, the combination of signal processing (e.g. WPA) and AI (e.g. SVM) provides high NDT performance.

Nevertheless, the high performance of SVM as a binary classifier with the realization of SVM as a multi-class classifier, N of SVM classifiers should be generated. This means one classifier for every single class. Therefore, during the training process, it should be considered that the data of the target class will be labeled as 1 and the rest of the data will be labeled as 0. This process will be repeated with each class to produce several classifiers that are capable to classify N classes. In the testing stage of SVM, the input data will be fed to all the classifiers to obtain the final result of classification. Therefore, in some cases, the input data may be classified into two or more classes which make the classification more confusion. Moreover, a large number of classes leads to a large number of classifiers. Therefore, this technique is time consuming due to high computation cost of a large number of SVM classifiers compared to the neural networks which build one network to classify several classes.

The compressive strength of concrete prediction is another application of AI-NDT to provide reliable inspection because of its importance in building maintenance and avoiding the collapse disasters. An approach of NDT is proposed in [83] to predict the compressive strength of concrete. The approach used two ultrasonic pulse transducers as transmitter and receiver to measure the wave velocity through the inspected materials and rebound hammer which is an elastic mass depends on the hardness of the surface mass strikes. The combination values of the two approaches are used to train SVM for estimation purpose. The experiment used a sample from 95 cylinder concrete, while the actual strength of each cylinder is used as a target result. The actual strength is measured in laboratory conditions using destructive compression tests. Then, ultrasonic pulse velocity and rebound hammer values are measured for the entire sample and 85 of them are used for the training process which labeled with their corresponding actual strength. The rest of the sample is used for a testing process to measure the estimation accuracy of concrete strength. The estimation result of SVM shows a promising

result compared to the statistical regression model. However, this method is not one side inspection and it can only be used to inspect accessible surfaces. Moreover, the actual strength of the concrete is measured using destructive compression tests where the sample is destroyed.

In the conventional NDT especially signal based techniques, the mathematics inversion of the back-scattered signals to characterize the defects in the inspected specimen still complicated to be achieved in real time due to the high computations cost of the nonlinear data. Therefore, the AI model such as support vector regression (SVR) can be proposed to achieve this task through learning by example even in an arbitrary form. A learning by example approach is introduced in [88] which aims to estimate the defect characteristic of a conductive surface such as position (e.g. x, y and z), length, depth and width based on SVR and eddy current signals. SVR is learned by labeling the real and imaginary parts of the eddy current frequency with a known defect's properties as an actual example. Therefore, in the inspection process, the real and imaginary parts of the eddy current frequency will be used to estimate unknown defect properties. In this approach, only the length and x parameters are tested and provide very good estimation result. This intelligence technique employs SVR to completely avoid the full mathematical modeling of the eddy currents for imaging the inspected specimen and provides real-time NDT.

Several advantages are provided using machine learning with conventional NDT techniques as shown in Table 5. In term of NDT automation, machine learning techniques such as ANN, DNN, SVM and SVR performed automatic NDT systems. The automation process aims to avoid the human error which is subjected to the inspector's individual experience. Moreover, NDT based on machine learning techniques such as [64] proposed to provide near to the real-time inspection which can speed up the production time. In addition, a reliable NDT is needed in reality to inspect the integrity of a product or structure. Therefore, the high accuracy rate is clearly achieved with NDT based on machine learning especially when several NDT techniques are integrated such as in [83] and [64]. The defect evaluation in [88], the use of machine learning in NDT provides valuable information about defect's position, length, depth and width to estimate the extent of the damage. On the other hand, two issues expose the machine learning techniques in NDT which are feature quality to improve the classifier performance and the size of the training sample. However, DNN in [58] aimed to optimize the features' quality by avoiding the manual features construction. The capability of ANN in [58] to be adopted by adjusting its weight hugely reduced the size of training samples which is difficult to be acquired in the real applications.

V. ARTIFICIAL INTELLIGENCE APPLICATIONS IN MICROWAVE NDT

Towards intelligent systems in NDT, AI based on machine learning approaches play a vital role in term of signal post-processing for defect detection and evaluation. AI can address the complexity of the collected data to improve the detection sensitivity of the defects [11]. In the conventional NDT techniques, machine learning approaches provide reliable and real-time inspection as well as avoiding complex mathematical modeling. However, the use of AI in microwave NDT (MNDT) still limited nevertheless its success in the other NDT techniques which high inspection accuracy is achieved. As mentioned, the microwave-based techniques have an advantage in inspecting both the conductive and non-conductive materials. Moreover, the microwave signals can penetrate the coating surface and interact with the inner layers which are affected by the variations of the thickness as well as due to the defect presence. Therefore, it necessitates enhancing the performance of MNDT techniques not only at the sensor design but also on the post-processing level. Therefore, the advanced integration between microwave signal processing and AI is needed to produce robust MNDT.

The earlier attempt to introduce intelligent MNDT was in [11] which aims to improve the OERW sensor sensitivity. The technique used a combination of SVM and ANN classifiers to find the small variations of the reflection coefficient which are difficult to be observed. Therefore, the high capability of the AI model to find small variations is used to be employed for improving the defect detection. The technique is employed to classify the coated steel specimens into defect and defect-free. The reflection coefficient is acquired from the defect and defect-free specimen and split into training and testing samples which are 46 and 369 samples respectively. The training samples are labeled into defect and defect-free. The frequency is swept from 12-18 GHz by 30 MHz increments using Vector Network Analyzer (VNA). As a result, 201 of frequency points are generated to be used as features. Each frequency point is normalized to its maximum value to mitigate the small stand-off variations. The frequency point vector is classified based on the features of principal component analysis (PCA). PCA is used to determine the significant features before they are used as input data for SVM and ANN. PCA uses a set of orthogonal transformations to represent the original sample into few uncorrelated values. Therefore, PCA is used for preprocessing the long features' vector to reduce the dimensionality of the features as well as selecting the most significant features to guide the classifiers. The higher accuracy rate (i.e. 99.62%) is achieved when only 13 PCA components are involved in the features vector. Nevertheless, the technique is limited to classify the inspected specimen into defect and defect-free without defect evaluation but the intelligent inspection achieves reliable defect detection even without considering the complicated noise preprocessing. Furthermore, the features normalization significantly improves the defect detection in the case of small stand-off variations.

An AI model can contribute more to MNDT because it is not limited to classify the inspected specimen into the defect and defect-free classes. Intelligent MNDT can achieve another task in defect evaluation such as defects imaging.

TABLE 5. Comparison summary of the machine learning techniques.

Ref. No.	Technique	Concept of use	Advantages	Disadvantages
[82]	ANN with ultrasonic velocities and rebound hardness values	Estimating the strength of concrete underwater.	- Robust estimation of concrete strength is achieved which is 98% by hybridizing ultrasonic velocities and rebound hardness techniques.	- A small sample set is used for the technique validation which leads to accuracy bias.
[60]	ANN with ultrasonic oscillogram and DWT coefficients	Automation of defect recognition process for stainless steel inspection.	- Automation of the NDT process for defect detection and recognition. - Reducing the training process using adjusting weight of untrained ANN. - The hybridization between signal processing technique (DWT) and artificial model (ANN) produces robust automatic inspection and 94% of recognition rate is achieved.	- The technique is limited for defect classification and does not provide any information about defects' size, depth and location.
[58]	DNN with ultrasonic images	Automation of ultrasonic image analysis process for NDT to classify stainless steel plates into defect and defect-free.	- DNN avoids the manual features construction and provides a quite simple structure compared to the conventional neural network. - 94.73% of classification accuracy is achieved because DNN provides a large margin between defect and defect-free classes.	- Massive training sample is needed to train the network. - The technique limited to visual features classification and it does not directly characterize ultrasonic echo waveform. - The technique is limited for defect and defect-free classification and does not recognize defect's type such as drilled hole and slit.
[64]	SVM with EC signals and WPA	Recognition aluminum alloys defects which are arc slots and inclined cracks.	- Online automatic inspection system. - The robust recognition rate is achieved which is 98.90%.	- The classification of a large number of defects' types, the system's speed will be degraded because extra SVM classifiers should be generated for multi-classification which increases the computations cost.
[83]	SVM with ultrasonic pulse velocities (UPV) and rebound hardness (RH)	Estimation of the compressive strength of concrete.	- Compared to the statistical regression model, a promising estimation result of concrete strength is achieved using SVM by hybridizing UPV and RH techniques with mean absolute percentage error 6.77% compared to the single input value of RH and UPV which are 8.92% and 9.25% respectively.	- Two sides' inspection which is limited to be used for an accessible structure. - Only 10 of the 95 samples are used in the validation process.
[88]	SVR with complex EC signals	Estimation of flow characteristics of a conductive surface.	- Inverse backscattering of EC signals is based on the estimation module. - Avoiding the mathematical modeling of EC for NDT imaging. - Various defect's characteristics are provided such as position, length, depth and width.	- The technique is based on learning by example which is needed for each new experiment because the geometrical characteristics of the flaws are not fixed.

The classification on the spatial level such as in [89] aims to classify the acquired signals into the defect and defect-free positions as well as to illustrate the defect position and size. The inspection is spatially performed using MTL sensor with SRR etched on the printed circuit board (PCB). The inspection is performed on a steel specimen to detect the corrosion underneath. The scanning achieved by 1 mm in x and y directions along with the inspected specimens. The magnitude of the transmission coefficient ($|S_{21}|$) is acquired at each inspected position. Each spatial point contains 191 frequency points through frequency sweeping from 3.25 GHz to 4.2 GHz by a 5MHz increment which is high dimensional features. Therefore, PCA is employed to reduce the features dimensional into 15 components. Each feature is labeled into the defected (1) and defect-free (0) regions and split into training and testing samples. The SVM classifier is employed to construct a 2D binary image by classifying each feature set into 1 and 0. The constructed image has clearly displayed the corrosion underneath which makes it capable to recognize the unseen corrosion position as well as to measure the corrosion size. However, there are several pixels wrongly represented as corrosion at the edges of corrosion regions. The false pixel classification is due to the absence of signal processing to eliminate the diffraction noise. Therefore, the integration between signal processing and AI model has been proven to provide reliable inspection as well as better resolution [59]. However, this technique is limited to evaluate only the defect location and size, while the defect depth cannot be estimated which is important to estimate the damage level. In addition, the features based on frequency sweeping lead to an increase in storage volume and time-consuming at the initial stage of the inspection [90]. Therefore, it is not

suitable for large structure inspection. Furthermore, feature dimensionality reduction technique such as PCA extracts the informative features set by mapping the original data set to a lower space. However, the features in the lower space do not correspond to the sweeping frequencies [91] which loss the original frequency points values.

In intelligent MNDT, features selection is another important factor to enhance the classifier performance as well as defect detection and evaluation. Generally, feature vector contains redundant values which are undesirable because they lead to an increase in the size of the feature vector and the processing time as well. Instead of performing the dimensionality reduction using PCA and loss the optimal frequency points representation as features, AI can be employed to select the most optimal frequency points to train a classifier and suppress the least important frequency points.

Two feature selection methods are applied in MNDT [92] which are Relief and Random Forest to find the most informative frequency point that can represent defects of a metallic plate based on the magnitude of the reflection coefficient. Relief algorithm [93] measures the relevance of a single feature in the problem space by increasing or decreasing its weight. On the other hand, the Random Forest algorithm [94] is recognized as a classifier which orders the importance of the features based on the classification accuracy [95]. The features are constructed as a tree and the nodes are randomly replaced to increase the classification accuracy. Both of the feature selection algorithms gave better classification accuracy against using a full features' vector. However, these techniques provide the most important features to be classified based on the analysis of the features first. The informative set of the features cannot be predictable to be used at the initial stage of the inspection process. Therefore, these techniques cannot avoid the storage issues and the long processing time in the initial stage of the implementation. Moreover, the classification accuracy based on the selected set of the frequency points is subject to be changed due to the stand-off variations which leads to change the optimal frequency points. Therefore, AI should be employed as a pattern recognition model to handle this challenge by auto-detection of the optimal frequency points.

Besides using the signals preprocessing techniques, statistical features, signal shape features and frequency points' features in NDT, there are several robust feature extractions algorithms can be used in MNDT applications in the future. Histogram of Oriented Gradients (HOG) is one of the best features extractor; it is widely used to describe edges and local shape information. It was introduced by Dalal and Triggs [96] to detect the human body by representing the objects based on the distribution of gradient intensities and orientations in spatially distributed regions. Moreover, the HOG provides strong orientation and illumination invariance and it is useful for recognizing objects' texture with deformable shapes [97] and small-scale changes [98]. Therefore, the capability of adapting HOG to be applied in MNDT should be investigated to extract defects' features for defect detection and recognition. However, HOG is limited to 8×8 pixels of the local region which is unsuitable for individual pixel classification such as the defected and defect-free pixels but it can be employed to classify the inspected specimens into the defected and defect-free. Moreover, HOG can be employed to describe various defects' shapes for defects recognition purpose.

Moreover, Local Binary Pattern (LBP) is another important descriptor introduced in [99] and shows high discriminative power in pattern recognition challenges. LBP represents a grey-scale image based on 3×3 non-overlapped blocks. Each block produces a single value based on the correlation between the center pixel value and its connecting pixels. The connecting pixels are considered as a binary number, where any pixel value less than the center pixel value is converted to 0 and otherwise converted to 1. As a result, a feature vector is constructed which can describe defect features in MNDT to represent the defected and defect-free regions of a spatial image. Similarly to HOG, LBP is limited to the local region with 3×3 pixels.

In addition, Gabor wavelets in [100] is another features extractor and have been widely used in image processing which provides better spatial domain and frequency domain resolution of 2D Gabor wavelet [101]. Furthermore, the use of Gabor wavelets has several advantages such as invariant to rotation and dilation with keeping the relationship among connecting pixels [102]. Therefore, in MNDT imaging, Gabor wavelets can be employed to extract the defect's features in various experiments' conditions to be applied in the future with regardless to the scaling and orientation variations of the captured image of the specimen under test.

Furthermore, besides ANN and SVM which are used in NDT, C4.5/J48 [103] is a statistical classifier which can be used in MNDT applications. C4.5/J48 builds a decision tree based on training dataset in both continuous and discrete features cases. The rules acquired from the generated tree are used to predict the class of testing data. The capability of the classifier to analyze huge data is high which used in data mining applications. J48 is the implementation of C4.5 classifier in the Weka data mining application. The classifier can take a decision in MNDT to classify the defected and defect-free specimens/positions whether for image-based features or signal based features.

Besides the contribution of AI in the conventional NDT, Table 6 shows the significant improvement of MNDT techniques based on AI techniques. The reliable defect detection with 100% of accuracy rate is achieved in [92] even without signal preprocessing. Moreover, few numbers of the raw features are involved in the detection process. Therefore, this result reflects the capability of microwave signals to improve classifier performance. The high capability of microwave signal to inspect the coated structure such as [11] provides a robust classification accuracy with 99.62% of accuracy rate. The high classification rate is because of the efficiency of microwave signals to interact with the inner layers of the compound structure. In addition, the integration between microwave and AI techniques in [89] provides innovative

TABLE 6. Comparison summary of AI-MNDT techniques.

Ref. No.	Technique	Concept of use	Advantages	Disadvantages
[11]	OERW with PCA, SVM and ANN.	Improving OERW sensor sensitivity for defect detection of the coated steel.	- The small stand-off variations are considered. - The significant features are selected using PCA and only 13 components are involved. - Reliable inspection is achieved with 99.62% of the accuracy rate.	- The technique does not provide defect evaluation. - Frequency sweeping technique leads to an increase in storage volume and time-consuming at the initial stage of the inspection. - PCA features losses the original value of the corresponding frequency point.
[89]	MTL and SRR with PCA and SVM classifier.	Corrosion underneath detection.	- The binary image is constructed to represent the defect size and location. - The significant features are selected using PCA and only 15 components are involved.	- High dimensional features are used at the initial stage which is 191 frequency points. - False detection is shown due to the absence of signal processing for de-noising. - The technique cannot be used to evaluate the defect depth.
[92]	Relief and Random Forest with SVM classifier.	Millimeter cracks detection in metallic surfaces.	- The normalized features are kept corresponding to their original frequency points. - 100% of accuracy rate is achieved using Random Forest and Relief with 5 and 11 features respectively compared to 97.10% using all features.	- The informative set of the features is unpredictable at the initial stage of the inspection.

defect evaluation in term of the defect size and position. Despite the modest attempts for integrating the microwave with AI techniques in NDT it performed encouraging result. Therefore, a further investigation in the future is required for full integration between AI and MNDT as well as to decrease the acquired data at the initial stage of microwave inspection.

VI. CONCLUSION

NDT techniques play vital roles in the industrial components during fabrication or in service to ensure the high production quality of products and early estimate harmful defects before causing the failure of the system. The performance of the conventional NDT techniques such as thermography, ultrasonic, eddy currents evaluation, X-ray and magnetic particles inspection is degraded due to the development of material sciences which produces complex structures of the manufactured material (e.g. composite materials and dielectric coating). Therefore, the trend of use MNDT for inspecting these structures rises up because the advantages of microwave-based techniques to handle conventional techniques' challenges. However, the conventional MNDT techniques still suffer numerous limitations such as blurred spatial images, intensive computations, and automation complexity.

Among conventional MNDT techniques, OERW is intensively used in the nondestructive inspection and shows a promising result in term of defects detection, localization and depth estimation of various materials such as metals, CFRP, GFRP, TBC and dielectric components. However, OERW based techniques face several challenges such as stand-off variations, optimal frequency point and poor quality images because researchers focus their research toward sensor-based enhancement with lack of implementation of soft computing techniques in MNDT applications.

Soft computing techniques such as preprocessing techniques, feature extraction techniques and machine learning classifiers aim to model and solve real challenges regardless of the mathematical complexity. Therefore, the prospect of using AI techniques in MNDT to solve the challenges of microwave-based techniques is possible to acquire an effective inspection result. For example, the high interference of the microwave diffracted waves between the sample surface and defect's edges leads to poor quality of OERW imaging and reflected on the measurement accuracy of defect sizing and depth. Therefore, putting this problem into a classification challenge using machine learning classifiers is possible to distinguish between the defected and defect-free regions. This is due to the high capability of machine learning techniques to train and solve complex and nonlinear data. Moreover, the accurate classification of the defected and defect-free regions will be reflected in the measurement accuracy of the defect evaluation in term of defect position and size.

In addition, as the capability of statistical machine learning techniques to estimate unknown value based on training set examples is high, therefore, statistical machine learning techniques can be employed to predict defect's depth based on known defects' examples. However, the performance of both classification and estimation of machine learning techniques are depending on the capability of the extracted features to describe defect position and its depth. Selecting right and unique features lead to improvement of the classifier accuracy and reduce processing time as well as to be suitable for real environment implementation. In this matter, a deep investigation is needed to transfer conventional feature extraction algorithms such as HOG and LBP from image processing domain into signal processing domain and their impact on MNDT efficiency.

The prospect of using signal processing techniques with AI approaches in MNDT is highly possible to enhance the efficiency of the inspection system because the impact AI is clearly seen in various fields such as pattern recognition, data mining and systems automation as well as the conventional NDT techniques. The use of AI in MNDT is not only restricted to overcome the above-mentioned challenges but also it can build automation system that capable to improve the production quality and monitoring during fabrication or in service and makes a qualitative difference in NDT applications. Moreover, the automation of MNDT tries avoiding the dependence on the skills and experience of the operators which decreases the possibility of the human error.

REFERENCES

[1] K. Manjula, K. Vijayarekha, and B. Venkatraman, "Weld flaw detection using various ultrasonic techniques: A review," *J. Appl. Sci.*, vol. 14, no. 14, pp. 1529–1535, 2014.

[2] L. S. Rosado, T. G. Santos, M. Piedade, P. M. Ramos, and P. Vilaça, "Advanced technique for non-destructive testing of friction stir welding of metals," *Measurement*, vol. 43, pp. 1021–1030, Oct. 2010.

[3] B. P. C. Rao, "Non-destructive testing and damage detection," in *Aerospace Materials and Material Technologies*. Singapore: Springer, 2017, pp. 209–228.

[4] H. Taheri, M. Kilpatrick, M. Norvalls, W. J. Harper, L. W. Koester, L. J. Bond, and T. Bigelow, "Investigation of nondestructive testing methods for friction stir welding," *Metals*, vol. 9, no. 6, p. 624, 2019.

[5] M. F. AJK, R. Sloan, C. I. Duff, M. Wielgat, and J. F. Knowles, "Nondestructive testing of thermal barrier coated turbine blades using microwave techniques," *Mater. Eval.*, vol. 74, no. 4, pp. 543–551, 2016.

[6] G. Davis, R. Nagarajah, S. Palanisamy, R. A. R. Rashid, P. Rajagopal, and K. Balasubramaniam, "Laser ultrasonic inspection of additive manufactured components," *Int. J. Adv. Manuf. Technol.*, vol. 102, nos. 5–8, pp. 2571–2579, 2019.

[7] A. Shukla, "Determination of elastic constants of Inconel-625 superalloy, using laser-based ultrasonic," *J. Theor. Appl. Phys.*, vol. 13, pp. 49–54, Mar. 2019.

[8] H. Zhang, B. Gao, G. Y. Tian, W. L. Woo, and L. Bai, "Metal defects sizing and detection under thick coating using microwave NDT," *NDT E Int.*, vol. 60, pp. 52–61, Dec. 2013.

[9] R. Zoughi, *Microwave Non-Destructive Testing and Evaluation Principles* vol. 4. Dordrecht, The Netherlands: Springer, 2012.

[10] M. Nesterov, T. Gagelmann, M. Bendler, S. Hantscher, S. Woeckel, and J. Auge, "Object reconstruction in non-destructive microwave defectoscopy," in *Proc. 19th ITG/GMA-Symp. Sensors Meas. Syst.*, 2018, pp. 1–4.

[11] A. Abdulbaset, H. Bing, and R. Omar, "Intelligent detection of cracks in metallic surfaces using a waveguide sensor loaded with metamaterial elements," *Sensors*, vol. 15, no. 5, pp. 11402–11416, May 2015.

[12] Z. Li, A. Haigh, C. Soutis, and A. Gibson, "Principles and applications of microwave testing for woven and non-woven carbon fibre-reinforced polymer composites: A topical review," *Appl. Compos. Mater.*, vol. 24, pp. 965–982, Aug. 2018.

[13] N. Samanian and M. Mohebbi, "Thermography, a new approach in food science studies: A review," *MOJ Food process Technol*, vol. 2, no. 3, pp. 110–119, 2016.

[14] F. Ciampa, P. Mahmoodi, F. Pinto, and M. Meo, "Recent advances in active infrared thermography for non-destructive testing of aerospace components," *Sensors*, vol. 18, no. 2, p. 609, Feb. 2018.

[15] A. Katunin, "A concept of thermographic method for non-destructive testing of polymeric composite structures using self-heating effect," *Sensors*, vol. 18, no. 1, p. 74, 2018.

[16] S. Deane, N. P. Avdelidis, C. Ibarra-Castanedo, H. Zhang, H. Y. Nezhad, T. Mackley, M. J. Davis, X. Maldague, A. Tsourdos, and A. A. Williamson, "Application of NDT thermographic imaging of aerospace structures," *Infr. Phys. Technol.*, vol. 97, pp. 456–466, Mar. 2019.

[17] N. Montinaro, D. Cerniglia, and G. Pitarresi, "Detection and characterisation of disbonds on fibre metal laminate hybrid composites by flying laser spot thermography," *Compos. B, Eng.*, vol. 108, pp. 164–173, Jan. 2017.

[18] J. García-Martín, J. Gómez-Gil, and E. Vázquez-Sánchez, "Non-destructive techniques based on eddy current testing," *Sensors*, vol. 11, no. 3, pp. 2525–2565, Feb. 2011.

[19] G. Bardl, R. Kupke, H. Heuer, and C. Cherif, "Eddy current testing in CFRP production," *Lightweight Des. Worldwide*, vol. 11, pp. 48–53, Feb. 2018.

[20] K. Mizukami, Y. Mizutani, A. Todoroki, and Y. Suzuki, "Detection of in-plane and out-of-plane fiber waviness in unidirectional carbon fiber reinforced composites using eddy current testing," *Compos. B, Eng.*, vol. 86, pp. 84–94, Feb. 2016.

[21] D. He, Z. Wang, M. Kusano, S. Kishimoto, and M. Watanabe, "Evaluation of 3D-printed titanium alloy using eddy current testing with high-sensitivity magnetic sensor," *NDT E Int.*, vol. 102, pp. 90–95, Mar. 2019.

[22] Z. Wang and Y. Yu, "Traditional eddy current–pulsed eddy current fusion diagnostic technique for multiple micro-cracks in metals," *Sensors*, vol. 18, no. 9, p. 2909, 2018.

[23] A. Lopez, R. Bacelar, I. Pires, T. G. Santos, J. P. Sousa, and L. Quintino, "Non-destructive testing application of radiography and ultrasound for wire and arc additive manufacturing," *Additive Manuf.*, vol. 21, pp. 298–306, May 2018.

[24] F. Zhong, C. Zhang, W. Li, J. Jiao, and L. Zhong, "Nonlinear ultrasonic characterization of intergranular corrosion damage in super 304H steel tube," *Anti-Corrosion Methods Mater.*, vol. 63, no. 2, pp. 145–152, 2016.

[25] Z. Li, J.-L. Yi, J.-L. Chen, and S. Hameed, "Ultrasonic Lamb waves applied in nondestractive damage evaluation," in *Proc. Symp. Piezoelectrcity, Acoustic Waves Device Appl. (SPAWDA)*, 2019, pp. 1–4.

[26] H. Jia, Z. Zhang, H. Liu, F. Dai, Y. Liu, and J. Leng, "An approach based on expectation-maximization algorithm for parameter estimation of Lamb wave signals," *Mech. Syst. Signal Process.*, vol. 120, pp. 341–355, Apr. 2019.

[27] E. L. M. Ribolla, M. R. Hajidehi, P. Rizzo, G. F. Scimemi, A. Spada, and G. Giambanco, "Ultrasonic inspection for the detection of debonding in CFRP-reinforced concrete," *Struct. Infrastruct. Eng.*, vol. 14, no. 6, pp. 807–816, 2018.

[28] J.-S. Lim, T.-S. Park, S.-J. Ha, and I.-K. Park, "Development of a multi-joint robotic ultrasonic inspection system to secure the integrity of composite structures," *J. Korean Soc. Nondestructive Test.*, vol. 38, no. 2, pp. 120–125, 2018.

[29] D. Cerniglia and N. Montinaro, "Defect detection in additively manufactured components: Laser ultrasound and laser thermography comparison," *Procedia Struct. Integr.*, vol. 8, pp. 154–162, 2018.

[30] R. Raišutis, E. Jasiūniene, R. Šliteris, and A. Vladišauskas, "The review of non-destructive testing techniques suitable for inspection of the wind turbine blades," *Ultragarsas*, vol. 63, no. 2, pp. 26–30, 2008.

[31] B. R. Müller, F. Léonard, A. Lange, A. Kupsch, and G. Bruno, "X-ray refraction techniques for fast, high-resolution microstructure characterization and non-destructive testing of lightweight composites," *Mater. Sci. Forum*, vols. 825–826, pp. 814–821, Jul. 2015.

[32] J. Zheng, Y. Shen, Z. Zhang, T. Wu, G. Zhang, and H. Lu, "Emerging wearable medical devices towards personalized healthcare," in *Proc. 8th Int. Conf. Body Area Netw.*, 2013, pp. 427–431.

[33] V. A. Klimenov, A. Buller, Y. Moskalev, S. Chakhlov, and M. Shteyn, "Mobile digital radiography system for nondestructive testing of large diameter pipelines," in *Proc. 18th World Conf. Non-Destructive Test.*, Durban, South Africa, Apr. 2012, pp. 16–20.

[34] I. Yulianti, A. Addawiyah, and R. Setiawan, "Optimization of exposure factors for X-ray radiography non-destructive testing of pearl oyster," *J. Phys., Conf. Ser.*, vol. 983, Mar. 2018, Art. no. 012004.

[35] S. Kolkoori, N. Wrobel, U. Zscherpel, and U. Ewert, "A new X-ray backscatter imaging technique for non-destructive testing of aerospace materials," *NDT E Int.*, vol. 70, pp. 41–52, Mar. 2015.

[36] Y. Deng and X. Liu, "Electromagnetic imaging methods for nondestructive evaluation applications," *Sensors*, vol. 11, no. 12, pp. 11774–11808, 2011.

[37] L. Zhiyong, Z. Qinlan, and L. Xiang, "New magnetic particle cassette NDT intelligent detection device," in *Proc. 4th Int. Conf. Intell. Syst. Design Eng. Appl.*, 2013, pp. 403–406.

[38] A. Zolfaghari, A. Zolfaghari, and F. Kolahan, "Reliability and sensitivity of magnetic particle nondestructive testing in detecting the surface cracks of welded components," *Nondestruct. Test. Eval.*, vol. 33, no. 3, pp. 290–300, 2018.

[39] E. Li, Y. Kang, and Y. Y. W. Wu, "Magnetic flux leakage testing method for micro-crack in bearings using magnetic inductive head probes," in *Electromagnetic Nondestructive Evaluation (XX)*, vol. 42. Amsterdam, The Netherlands: IOS Press, 2017, pp. 25–31.

[40] A. Sadr and R. S. Okhovat, "Extracting the region of interest from MFL signals," *Turkish J. Elect. Eng. Comput. Sci.*, vol. 24, pp. 427–434, Jan. 2016.

[41] A. Todoroki, K. Yamada, Y. Mizutani, Y. Suzuki, and R. Matsuzaki, "Impact damage detection of a carbon-fibre-reinforced-polymer plate employing self-sensing time-domain reflectometry," *Compos. Struct.*, vol. 130, pp. 174–179, Oct. 2015.

[42] Z. Li, A. Haigh, C. Soutis, A. Gibson, and R. Sloan, "Applications of microwave techniques for aerospace composites," in *Proc. IEEE Int. Conf. Microw., Antennas, Commun. Electron. Syst. (COMCAS)*, Nov. 2017, pp. 1–4.

[43] R. Rajni, A. Kaur, and A. Marwaha, "Complementary split ring resonator based sensor for crack detection," *Int. J. Electr. Comput. Eng.*, vol. 5, Oct. 2015, pp. 1012–1017.

[44] J.-C. Bolomey, "Recent European developments in active microwave imaging for industrial, scientific, and medical applications," *IEEE Trans. Microw. Theory Techn.*, vol. 37, no. 12, pp. 2109–2117, Dec. 1989.

[45] P. Butz, C. Hofmann, and B. Tauscher, "Recent developments in noninvasive techniques for fresh fruit and vegetable internal quality analysis," *J. Food Sci.*, vol. 70, pp. R131–R141, Nov. 2005.

[46] A. Franchois and C. Pichot, "Microwave imaging-complex permittivity reconstruction with a Levenberg–Marquardt method," *IEEE Trans. Antennas Propag.*, vol. 45, no. 2, pp. 203–215, Feb. 1997.

[47] S. Kon, K. Watabe, and M. Horibe, "Nondestructive method using transmission line for detection of foreign objects in food," in *Proc. IEEE Sensors Appl. Symp. (SAS)*, Mar. 2018, pp. 1–4.

[48] Z. Li, A. Haigh, C. Soutis, A. Gibson, and R. Sloan, "Evaluation of water content in honey using microwave transmission line technique," *J. Food Eng.*, vol. 215, pp. 113–125, Jul. 2017.

[49] A. M. Albishi, O. M. Ramahi, and M. S. Boybay, "Complementary split-ring resonator as a high sensitivity sensor," in *Proc. IEEE Antennas Propag. Soc. Int. Symp. (APSURSI)*, Jul. 2012, pp. 1–2.

[50] Z. Li and Z. Meng, "A review of the radio frequency non-destructive testing for carbon-fibre composites," *Meas. Sci. Rev.*, vol. 16, no. 2, pp. 68–76, Apr. 2016.

[51] A. Trakic, Y. Wang, D. Foster, and A. Abbosh, "Microwave split-ring resonator array for imaging of near-surface material defects," in *Proc. Austral. Microw. Symp. (AMS)*, 2018, pp. 47–48.

[52] M. F. Akbar, G. N. Jawad, L. R. Danoon, and R. Sloan, "Delamination detection in glass-fibre reinforced polymer (GFRP) using microwave time domain reflectometry," in *Proc. 15th Eur. Radar Conf. (EuRAD)*, 2018, pp. 253–256.

[53] B. Salski, W. Gwarek, and P. Korpas, "Electromagnetic inspection of carbon-fiber-reinforced polymer composites with coupled spiral inductors," *IEEE Trans. Microw. Theory Techn.*, vol. 62, no. 7, pp. 1535–1544, Jul. 2014.

[54] S. Guorong, Y. Tianting, H. Cunfu, Y. Shen, L. Yan, and W. Bin, "Detection of surface crack on the substrate under thermal barrier coatings using microwave non-destructive evaluation," *J. Microw. Power Electromagn. Energy*, vol. 49, no. 2, pp. 69–75, 2015.

[55] A. J. K. M. Firdaus, R. Sloan, C. I. Duff, M. Wielgat, and J. F. Knowles, "Microwave nondestructive evaluation of thermal barrier coated turbine blades using correlation analysis," in *Proc. 46th Eur. Microw. Conf. (EuMC)*, 2016, pp. 520–523.

[56] M. D. Buhari, G. Y. Tian, and R. Tiwari, "Microwave-based SAR technique for pipeline inspection using autofocus range-Doppler algorithm," *IEEE Sensors J.*, vol. 19, no. 5, pp. 1777–1787, Mar. 2019.

[57] N. Munir, H.-J. Kim, S.-J. Song, and S.-S. Kang, "Investigation of deep neural network with drop out for ultrasonic flaw classification in weldments," *J. Mech. Sci. Technol.*, vol. 32, pp. 3073–3080, 2018.

[58] J. Ye, S. Ito, and N. Toyama, "Computerized ultrasonic imaging inspection: From shallow to deep learning," *Sensors*, vol. 18, no. 11, p. 3820, 2018.

[59] M. S. M. Naqiuddin, M. S. Leong, L. M. Hee, and M. A. M. Azrieasrie, "Ultrasonic signal processing techniques for pipeline: A review," in *Proc. MATEC Web Conf.*, 2019, p. 6006.

[60] S. Sambath, P. Nagaraj, and N. Selvakumar, "Automatic defect classification in ultrasonic NDT using artificial intelligence," *J. Nondestruct. Eval.*, vol. 30, pp. 20–28, Mar. 2011.

[61] R. D. Tipones and J. C. D. Cruz, "Design and development of a material impact tester using neural network for concrete ratio classification," in *Proc. IEEE 13th Int. Colloq. Signal Process. Appl. (CSPA)*, Mar. 2017, pp. 106–111.

[62] K. A. Tiwari, R. Raisutis, and V. Samaitis, "Signal processing methods to improve the Signal-to-noise ratio (SNR) in ultrasonic non-destructive testing of wind turbine blade," *Procedia Struct. Integr.*, vol. 5, no. 5, pp. 1184–1191, 2017.

[63] R. W. Schafer and A. V. Oppenheim, *Discrete-Time Signal Processing* (Prentice-Hall Signal Processing Series). Englewood Cliffs, NJ, USA: Prentice-Hall, 1989.

[64] B. Liu, D. Hou, P. Huang, B. Liu, H. Tang, and W. Zhang, "An improved PSO-SVM model for online recognition defects in eddy current testing," *Nondestruct. Test. Eval.*, vol. 28, pp. 367–385, Dec. 2013.

[65] A. T. Farid, "Prediction of unknown deep foundation lengths using the Hilbert Huang Transform (HHT)," *HBRC J.*, vol. 8, pp. 123–131, Aug. 2012.

[66] N. F. Giannelis, A. J. Murray, and G. A. Vio, "Application of the Hilbert–Huang Transform in the identification of frequency synchronisation in transonic aeroelastic systems," in *Proc. AIAA Scitech Forum*, 2019, p. 1341.

[67] F. Li, R. Li, L. Tian, L. Chen, and J. Liu, "Data-driven time-frequency analysis method based on variational mode decomposition and its application to gear fault diagnosis in variable working conditions," *Mech. Syst. Signal Process.*, vol. 116, pp. 462–479, Feb. 2019.

[68] M. E. Abdulmunem and A. A. Badr, "Hilbert transform and its applications: A survey," *Int. J. Sci. Eng. Res.*, vol. 8, pp. 699–704, Feb. 2017.

[69] C. A. Sciammarella, L. Lamberti, and F. M. Sciammarella, "The optical signal analysis (OSA) method to process fringe patterns containing displacement information," *Opt. Lasers Eng.*, vol. 115, pp. 225–237, Apr. 2019.

[70] C. Polat and M. S. Özerdem, "Introduction to Wavelets and their applications in signal denoising," *Bitlis Eren Univ. J. Sci. Technol.*, vol. 8, no. 1, pp. 1–10, 2018.

[71] D. Gupta and S. Choubey, "Discrete wavelet transform for image processing," *Int. J. Emerg. Technol. Adv. Eng.*, vol. 4, pp. 598–602, Mar. 2015.

[72] M. Gowri S. G. and C. Prasanna Raj P., "Energy density feature extraction using different wavelets for emotion detection," *Int. J. Appl. Eng. Res.*, vol. 13, no. 1, pp. 520–527, 2018.

[73] W. Zhang, L. Sun, and L. Zhang, "Local damage identification method using finite element model updating based on a new wavelet damage function," *Adv. Struct. Eng.*, vol. 21, no. 10, pp. 1482–1494, 2018.

[74] S. Kamal and C. Kaur, "Design of vedic multiplier in image compression and FPGA implementation using discrete wavelet transform (DWT) algorithm," *Int. J. Eng. Sci.*, vol. 6, no. 3, pp. 2259–2262, 2016.

[75] I. A. Sawaneh, "An effective method for e-medical data compression using wavelet analysis," *Imaging*, vol. 6, no. 3, pp. 25–32, 2018.

[76] N. Bessous, S. E. Zouzou, W. Bentrah, S. Sbaa, and M. Sahraoui, "Diagnosis of bearing defects in induction motors using discrete wavelet transform," *Int. J. Syst. Assurance Eng. Manage.*, pp. 1–9, 2018.

[77] P. J. Navarro, C. Fernández-Isla, P. Alcover, and J. Suardíaz, "Defect detection in textures through the use of entropy as a means for automatically selecting the wavelet decomposition level," *Sensors*, vol. 16, p. 1178, Jul. 2016.

[78] D.-M. Cui, W. Yan, X.-Q. Wang, and L.-M. Lu, "Towards intelligent interpretation of low strain pile integrity testing results using machine learning techniques," *Sensors*, vol. 17, p. 2443, Nov. 2017.

[79] V. Matz, M. Kreidl, and R. Smid, "Classification of ultrasonic signals," *Int. J. Mater. Product Technol.*, vol. 27, pp. 145–155, Oct. 2006.

[80] P. Yang and Q. Li, "Wavelet transform-based feature extraction for ultrasonic flaw signal classification," *Neural Comput. Appl.*, vol. 24, pp. 817–826, Mar. 2014.

[81] W. Nash, T. Drummond, and N. Birbilis, "A review of deep learning in the study of materials degradation," *NPJ Mater. Degradation*, vol. 2, Nov. 2018, Art. no. 37.

[82] S. Park, J. Kim, E. Shin, and S. Han, "Compressive strength evaluation of underwater concrete structures integrating the combination of rebound hardness and ultrasonic pulse velocity methods with artificial neural networks," *Int. J. Civil Environ. Struct. Constr. Architect. Eng.*, vol. 8, no. 1, pp. 17–21, 2014.

[83] Y.-F. Shih, Y.-R. Wang, K.-L. Lin, and C.-W. Chen, "Improving non-destructive concrete strength tests using support vector machines," *Materials*, vol. 8, pp. 7169–7178, Oct. 2015.

[84] D. A. Winkler, "Deep and shallow neural networks," in *Chemoinformatics: Basic Concepts and Methods*. Weinheim, Germany: Wiley, 2018, p. 453.
[85] N. Munir, H.-J. Kim, J. Park, S.-J. Song, and S.-S. Kang, "Convolutional neural network for ultrasonic weldment flaw classification in noisy conditions," *Ultrasonics*, vol. 94, pp. 74–81, Apr. 2019.
[86] A. P. Castaño, "Support vector machines," in *Practical Artificial Intelligence*. Berkeley, CA, USA: Apress, 2018, pp. 315–365.
[87] A. Prosvirin, J. Kim, and J.-M. Kim, "Efficient rub-impact fault diagnosis scheme based on hybrid feature extraction and SVM," in *Advances in Computer Communication and Computational Sciences*. Singapore: Springer, 2019, pp. 405–415.
[88] M. Salucci, G. Oliveri, F. Viani, R. Miorelli, C. Reboud, A. Massa, and P. Calmon, "A learning-by-examples approach for non-destructive localization and characterization of defects through eddy current measurements," in *Proc. IEEE Int. Symp. Antennas Propag. USNC/URSI Nat. Radio Sci. Meeting*, Jul. 2015, pp. 900–901.
[89] A. Ali, A. Albasir, and O. M. Ramahi, "Microwave sensor for imaging corrosion under coatings utilizing pattern recognition," in *Proc. IEEE Int. Symp. Antennas Propag. (APSURSI)*, Jun./Jul. 2016, pp. 951–952.
[90] L. Li, X. Yang, Y. Yin, J. Yuan, X. Li, and L. Li, "An interdigital electrode probe for detection, localization and evaluation of surface notch-type damage in metals," *Sensors*, vol. 18, p. 371, Jan. 2018.
[91] A. Moomen, A. Ali, and O. Ramahi, "Reducing sweeping frequencies in microwave NDT employing machine learning feature selection," *Sensors*, vol. 16, p. 559, Apr. 2016.
[92] A. Ali, O. M. Ramahi, and A. Mooman, "Optimizing sweeping frequencies of microwave sensors using intelligent feature selection," in *Proc. IEEE Int. Symp. Antennas Propag. (APSURSI)*, Jun./Jul. 2016, pp. 1957–1958.
[93] I. Kononenko, "Estimating attributes: Analysis and extensions of RELIEF," in *Proc. Eur. Conf. Mach. Learn.*, 1994, pp. 171–182.
[94] L. Breiman, "Random forests," *Mach. Learn.*, vol. 45, no. 1, pp. 5–32, 2001.
[95] L. Čehovin and Z. Bosnić, "Empirical evaluation of feature selection methods in classification," *Intell. Data Anal.*, vol. 14, no. 3, pp. 265–281, 2010.
[96] N. Dalal and B. Triggs, "Histograms of oriented gradients for human detection," in *Proc. IEEE Comput. Soc. Conf. Comput. Vis. Pattern Recognit. (CVPR)*, Jun. 2005, pp. 886–893.
[97] G. Cheng and J. Han, "A survey on object detection in optical remote sensing images," *ISPRS J. Photogramm. Remote Sens.*, vol. 117, pp. 11–28, Jul. 2016.
[98] A. V. Vokhmintcev, I. V. Sochenkov, V. V. Kuznetsov, and D. V. Tikhonkikh, "Face recognition based on a matching algorithm with recursive calculation of oriented gradient histograms," *Doklady Math.*, vol. 93, pp. 37–41, Jan. 2016.
[99] T. Ojala, M. Pietikäinen, and D. Harwood, "A comparative study of texture measures with classification based on featured distributions," *Pattern Recognit.*, vol. 29, no. 1, pp. 51–59, 1996.
[100] J. G. Daugman, "Complete discrete 2-D Gabor transforms by neural networks for image analysis and compression," *IEEE Trans. Acoust., Speech Signal Process.*, vol. ASSP-36, no. 7, pp. 1169–1179, Jul. 1988.
[101] S. Zeng, L. Chen, L. Jiang, and C. Gao, "Hyperspectral imaging technique based on Geodesic K-medoids clustering and Gabor wavelets for pork quality evaluation," *Int. J. Wavelets, Multiresolution Inf. Process.*, vol. 15, no. 6, 2017, Art. no. 1750066.
[102] H. S. Mohan and A. R. Reddy, "Face recognition using Gabor wavelet networks," in *Proc. Nat. Conf. Recent Trends Electron. Commun. (NCRTEC)*, 2008, pp. 1–7.
[103] G. H. John, "Robust linear discriminant trees," in *Learning From Data*. New York, NY, USA: Springer, 1996, pp. 375–385.

NAWAF H. M. M. SHRIFAN received the bachelor's degree in computer science and engineering from the University of Aden, Aden, Yemen, in 2006, and the M.Sc. degree in informatics from Universiti Sains Malaysia (USM), Nibong Tebal, Malaysia, in 2017, where he is currently pursuing the Ph.D. degree in microwave nondestructive testing with the School of Electrical and Electronic Engineering. He is also a Lecturer with the Faculty of Oil and Minerals, University of Aden.

MUHAMMAD FIRDAUS AKBAR (GS'16–M'18) received the B.Sc. degree in communication engineering from International Islamic University Malaysia (IIUM), Malaysia, in 2010, and the M.Sc. and Ph.D. degree from The University of Manchester, Manchester, U.K, in 2012 and 2018, respectively. From 2010 to 2011, he was with Motorola Solutions, Pulau Pinang, Malaysia, as a Research and Development Engineer. From 2012 to 2014, he was an Electrical Engineer with Usains Infotech Sdn Bhd, Penang, Malaysia. He is currently a Senior Lecturer with Universiti Sains Malaysia (USM). His current research interests include electromagnetics, microwave nondestructive testing, microwave sensor, and imaging.

NOR ASHIDI MAT ISA received the B.Eng. degree (Hons.) in electrical and electronic engineering from Universiti Sains Malaysia (USM), in 1999, and the Ph.D. degree in electronic engineering (majoring in image processing and artificial neural networks). He is currently a Professor and the Deputy Dean of academic, career and international with the School of Electrical and Electronic Engineering, USM. His research interests include intelligent systems, image processing, neural networks, biomedical engineering, and intelligent diagnostic systems and algorithms.